ITTC Quality System Manual
Recommended Procedures and Guidelines

Procedure

Estimation of Roll Damping

7.5	Process Control
7.5-02	Testing and Extrapolation Methods
7.5-02-07	Loads and Responses
7.5-02-07-04	Stability
7.5-02-07-04.5	Estimation of Roll Damping

Updated / Edited by	Approved
Stability in Waves Committee of the 30th ITTC	30th ITTC 2024
Date 04/2024	Date 09/2024

Table of Contents

Estimation of Roll Damping

1. PURPOSE OF PROCEDURE

Roll damping is, in general, the energy that a system dissipates when rolling, which is a crucial parameter for the proper estimation of the ship behaviour in a seaway. Traditionally, the most common practice to obtain roll damping is to perform the roll decay test. With the development of model testing techniques, more sophisticated methods such as free running forced roll tests and (semi-) captive forced roll tests become available to help investigate the more detailed characteristics of roll damping as the function of frequency and amplitude. These methods can also be useful for CFD validation purposes.

This procedure provides detailed guidance on how to carry out model tests, or using empirical formula, to determine roll damping:

- Roll decay tests in calm water
- Free running forced roll tests
- (Semi-) Captive forced roll tests
- Simplified Ikeda's method
- Ikeda's method

Roll decay tests in waves are performed occasionally but are not included in this procedure, reference can be found in literature (Tao et al, 2005).

2. BACKGROUND EQUATIONS

In this section, the equation of ship roll motion is presented. Then, the general formulation to model the restoring moment is illustrated. Lastly, some of the expressions commonly used to model roll damping are introduced, along with the review of the relations among them.

2.1 Equation of ship roll motion

Ship motions can be expressed in six-degrees-of freedom. Roll motion, specifically, is the rotation of the ship around the longitudinal axis, which is coupled to sway and yaw motions. However, coupling of roll with other degrees of freedom is generally neglected because a good balance is achieved between simplicity and accuracy when using one degree-of-freedom, although it should be decided on a specific ship hull basis.

To begin with, a generic formulation is expressed in order to introduce the roll damping formulation. However, it should be noted that the specific equation of ship roll motion used to analyse the tests in this procedure should be carefully established in order to properly model the physics involved.

In the following, in order to discuss the problem of nonlinear roll damping, the equation of ship roll motion is expressed in the simple single-degree-of-freedom form:

$$(I_{44} + \partial I_{44}) \cdot \ddot{\varphi} + B(\dot{\varphi}) + C_{44} = K \tag{1}$$

where φ $[rad]$ is the roll angle (dots represent derivatives with respect to time); t $[s]$ is time, $(I_{44} + \partial I_{44})$ $[kg \cdot m^2]$ is the total roll moment of inertia, including the hydrodynamic added inertia (∂I_{44}) along a longitudinal axis through the centre of gravity; $B(\dot{\varphi})$ $[N \cdot m]$ is the damping moment function, assumed to be dependent only on the ship's roll angular velocity; C_{44} $[N \cdot m]$ is the restoring moment and K $[N \cdot m]$ is the exciting roll moment applied to the ship due to waves or external/internal forces.

Dividing Eq.(1) by $(I_{44} + \partial I_{44})$, the so-called normalized roll motion equation (IMO, 2006) can be obtained:

$$\ddot{\varphi} + d(\dot{\varphi}) + c_{44} = k \tag{2}$$

where:

$$d(\dot{\varphi}) = \frac{B(\dot{\varphi})}{(I_{44}+\partial I_{44})}, \quad c_{44} = \frac{C_{44}}{(I_{44}+\partial I_{44})}, \quad k = \frac{K}{(I_{44}+\partial I_{44})} \tag{3}$$

2.2 Restoring coefficients

The restoring moment, C_{44}, can be expressed in the following nonlinear form:

$$C_{44} = \Delta \cdot \overline{GZ}(\varphi) \tag{4}$$

where Δ $[N]$ is the ship displacement and $\overline{GZ}(\varphi)$ $[m]$ is the hydrostatic roll righting lever with respect to the centre of gravity of the ship.

Because of Eq. (4), and considering Eq. (2), c_{44} is equivalent to:

$$c_{44} = \omega_x^2 \cdot \frac{\overline{GZ}(\varphi)}{\overline{GM}} = \omega_x^2 \cdot r(\varphi) \tag{5}$$

where $\omega_x [rad/s]$ represents the undamped ship roll natural frequency and $\overline{GM}$ $[m]$ is the metacentric height with respect to the ship centre of gravity, considering the vessel freely floating with displacement Δ.

For symmetric ships symmetrically loaded, where $\overline{GZ}(\varphi)$ is symmetric around $\varphi = 0$, $r(\varphi)$ may be considered to be a polynomial, generally an odd polynomial. The general form of $r(\varphi)$ is as follows:

$$r(\varphi) = \sum_{n=1,3,5,\dots} \gamma_n \cdot \varphi^n \quad \text{with } \gamma_1 = 1 \tag{6}$$

For a specific ship hull and loading condition, if the hydrostatic roll righting lever ($\overline{GZ}(\varphi)$) presents a linear behaviour for the range of expected and/or tested rolling angles, the restoring moment may be considered linear and, therefore, be defined as:

$$C_{44} = \Delta \cdot \overline{GM} \tag{7}$$

corresponding to $r(\varphi)$=1 in Eq. (5).

2.3 Roll damping coefficients

Roll damping coefficients can be expressed in many ways, for example, in the linear or non-linear form. The damping moment function $D(\dot{\varphi})[N \cdot m]$can be expressed following a non-linear representation as a series expansion of $\dot{\varphi}$ and $|\dot{\varphi}|$ in the form:

$$B(\dot{\varphi}) = B_{\varphi,1} \cdot \dot{\varphi} + B_{\varphi,2} \cdot \dot{\varphi} \cdot |\dot{\varphi}| + B_{\varphi,3} \cdot \dot{\varphi}^3 + \dots \tag{8}$$

The $B_{\varphi,1}$ $[N \cdot m \cdot s]$, $B_{\varphi,2} [N \cdot m \cdot s^2]$, $B_{\varphi,3}$ $[N \cdot m \cdot s^3]$, etc. in Eq.(8) are the nonlinear damping components and are considered constants during the steady periodic oscillation concerned, which are characterized by the steady rolling amplitude φ_a and the steady periodic oscillation ω_E. It should be noted that these coefficients may not be the same values for a different steady periodic oscillation, so, they may depend on the amplitude φ_a and the frequency ω_E of steady periodic oscillation.

Among all the available mathematical models of nonlinear roll damping, the most typical is the linear-quadratic-cubic damping model, whose expression is (Bulian, 2004):

$$d(\dot{\varphi}) = 2 \cdot \mu \cdot \dot{\varphi} + \beta \cdot \dot{\varphi} \cdot |\dot{\varphi}| + \delta \cdot \dot{\varphi}^3 \tag{9}$$

where μ $[1/s]$, β $[-]$ and δ $[s]$ are the linear, quadratic and cubic damping components, respectively. Also, depending on the ship hull and on the presence of bilge keels, the linear-quadratic ($\delta = 0$) or linear-cubic ($\beta = 0$) damping models may be considered as well.

The relationship between μ, β, δ and $B_{\varphi,1}$, $B_{\varphi,2}$, $B_{\varphi,3}$ is as follows:

$$\mu = \frac{B_{\varphi,1}}{2\cdot(I_{44}+\partial I_{44})};\quad \beta = \frac{B_{\varphi,2}}{(I_{44}+\partial I_{44})} \quad \delta = \frac{B_{\varphi,3}}{(I_{44}+\partial I_{44})} \tag{10}$$

2.4 Equivalent linear damping coefficient

Since it is difficult to analyse strictly the nonlinear equation stated in Eq. (1), or the analogous Eq. (2), when considering the nonlinear damping formulation, as no analytical solution exist, Parametric Identification Techniques (PIT) should be used or, alternatively, the nonlinear damping model may be replaced by linearized damping model in a limited time window, as follows:

$$\begin{cases} B(\dot{\varphi}) = B_{eq}\cdot\dot{\varphi} \\ d(\dot{\varphi}) = 2\cdot\mu_{eq}\cdot\dot{\varphi} \end{cases} \tag{11}$$

where $B_{eq}[(N\cdot m)/s]$ denotes the equivalent linear damping component and μ_{eq} $[1/s]$ the equivalent linear damping coefficient per unit mass moment of inertia $B_{eq}/\left(2\cdot(I_{44}+\partial I_{44})\right)$.

There are several ways to express the equivalent linear damping coefficient in terms of the nonlinear damping coefficients. Prior to determine their relationship, a specific mathematical model of roll damping must be assumed, such as the one presented in Eq. (9). The most general way to relate the nonlinear damping coefficients and the equivalent linear damping coefficient is to assume that the energy loss due to damping during a half cycle of roll is the same when nonlinear and linear damping are used (Tasai, 1965; Bulian et al., 2009).

If the roll motion is assumed to be a steady periodic oscillation with its amplitude ϕ_a and its circular frequency ω_E, the relationship between them is defined by a parametric model which may be obtained by requiring, in a least squares sense, the following:

$$\begin{cases} \int_0^{2\cdot\pi/\omega_E} 2\cdot\mu_{eq}\cdot\dot{\varphi}^2 dt = \int_0^{2\cdot\pi/\omega_E} d(\dot{\varphi})\cdot\dot{\varphi}dt \\ \dot{\varphi} = \varphi_a\cdot\omega_E\cdot\sin(\omega_E\cdot t) \end{cases} \tag{12}$$

Applying the previous equation, considering the nonlinear damping model of Eq. (9), the relationship between μ_{eq} and μ, β and δ is represented by the following parametric model:

$$\begin{cases} \mu_{eq}(\varphi_a) = \mu + \frac{4}{3\cdot\pi}\cdot\beta\cdot(\omega_E(\varphi_a)\cdot\varphi_a) + \\ \frac{3}{8}\cdot\delta\cdot(\omega_E(\varphi_a)\cdot\varphi_a)^2 \\ \omega_E(\varphi_a) = \sqrt{\omega_{x,eq}^2(\varphi_a) - \mu_{eq}^2(\varphi_a)} \end{cases} \tag{13}$$

where $\omega_{x,eq}$ $[rad/s]$ is the equivalent undamped roll natural frequency, which when considering the nonlinear restoring expressed in Eq. (5), may be determined by:

$$\omega_{x,eq}^2(\varphi_a) = \frac{\omega_x^2}{\overline{GM}} \cdot \frac{\int_0^{2\cdot\pi}\overline{GZ}(\varphi=\varphi_a\cdot\cos(\alpha))\cdot\cos(\alpha)d\alpha}{\pi\cdot\varphi_a} \tag{14}$$

If the nonlinear restoring is not considered, then simply the equivalent undamped roll natural frequency $\omega_{x,eq}$ is equal to the undamped roll natural frequency ω_x.

From Eq. (11) and Eq. **Errore. L'origine riferimento non è stata trovata.**, the equivalent linear damping component may be derived:

$$B_{\mathrm{eq}} = B_{\varphi,1} + \frac{8}{3\cdot\pi}\cdot(\omega_{\mathrm{E}}\cdot\varphi_{\mathrm{a}})\cdot B_{\varphi,2} + \frac{3}{4}\cdot(\omega_{\mathrm{E}}\cdot\varphi_{\mathrm{a}})^2\cdot B_{\varphi,3} \tag{15}$$

For more general periodic motion, the parametric model of roll damping can be derived by equating the first terms of the Fourier expansions of Eqs.(11) and (8) (Takaki *et al*, 1973).

In the case of irregular roll motion, the linearization of the roll damping expression, following the work of Kaplan (1966), Vassilopoulos (1971) and others, may be done by assuming that the difference of the damping moment between its linearized and nonlinear forms can be minimized in the sense of the least squares method. Also, making the further assumptions that the undulation of the roll angular velocity $\dot{\varphi}$ is subject to a Gaussian process and that the damping coefficients remain constant. Considering the linear-quadratic-cubic damping model (JSRA, 1977; Oliveira et al., 2018):

$$\begin{cases} \chi_d = 2 \cdot \mu \cdot \dot{\varphi} + \beta \cdot |\dot{\varphi}| + \delta \cdot \dot{\varphi}^3 - 2 \cdot \mu_{\mathrm{eq}} \cdot \dot{\varphi} \\ \dfrac{\partial \chi_d^2}{\partial \mu_{\mathrm{eq}}} = 0 \end{cases} \tag{16}$$

The relationship between the linearized roll damping coefficient and the nonlinear damping coefficients is:

$$\begin{cases} \mu_{eq}(\sigma_{\dot{x}}) = \mu + \sqrt{\dfrac{2}{\pi}} \cdot \beta \cdot \sigma_{\dot{x}} + \dfrac{3}{2} \cdot \delta \cdot \sigma_{\dot{x}}{}^2 \\ B_{eq}(\sigma_{\dot{x}}) = B_{\varphi,1} + \sqrt{\dfrac{8}{\pi}} \cdot B_{\varphi,2} \cdot \sigma_{\dot{x}} + 3 \cdot B_{\varphi,3} \cdot \sigma_{\dot{x}}{}^2 \end{cases} \tag{17}$$

where $\sigma_{\dot{x}}[rad/s]$ represents the standard deviation of the roll velocity $\dot{\varphi}$.

Another form of expressing the linearized roll damping coefficient is the Bertin's extinction coefficient $N(\varphi_a)$ or also called "N-coefficient" (Bertin, 1874a, 1874b; Motora, 1964). The relationship between the Bertin's expression and the equivalent linear roll damping coefficient is as follows:

$$\mu_{eq}(\varphi_a) = \frac{1}{\pi} \cdot N(\varphi_a) \cdot \varphi_a \cdot \omega_x \tag{18}$$

with φ_a in radians

The N-coefficient may be used to process the decaying curves of a roll decay tests, as exemplified in the MSC.1/Circ. 1200 (IMO, 2006). Note that the value φ_a is in degrees in MSC.1/Circ. 1200.

Caution should be taken not to double count the wave making component of roll damping when numerical computations are carried out using potential codes, as described in ITTC Recommended Procedure 7.5-02-07-04.3, see also (France et al. 2003).

3. PROCEDURE FOR ESTIMATING ROLL DAMPING FROM EXPERIMENTS

The procedures proposed herein are intended to provide a basis to carry out roll decay and forced roll tests, for a hull fitted with or without appendages and for each loading condition. They may be subject to modifications on a specific case base. The procedures are based on the IMO MSC.1/Circ. 1200 (IMO, 2006) and on the IMO SLF 47/6/8 (IMO, 2004) document.

Scale effects of roll damping have not been considered in the procedure, although some guidelines are provided to avoid them. Some information on this regard may be found in the literature (e.g. Gawn, 1940; Bertgalia et al., 2004; Bulian et al., 2009; Söder et al., 2012; Handschel et al., 2014b), but further studies are required to overcome the roll damping extrapolation and fully understand the scale effects.

When experimentally determined roll damping coefficients are used in numerical calculations, care should be taken to validate that numerical code determines the same rolling amplitudes as the experiments when assuming the same hydrodynamic scenario.

3.1 Roll decay tests in calm water

Roll decay tests are based on inducing an initial heel to the ship model, releasing it allowing to roll freely, and then recording and analysing the transitory roll motion, i.e. the decaying oscillations.

Roll decay tests may be performed with and without forward speed. If the tests are carried out with forward speed, the roll damping derived from them may be different to the roll damping from roll decays tests without forward speed and, generally, larger. Furthermore, it should be considered that, when performing the test with forward speed, the model needs to be either towed or free running. If the model is towed, special attention should be paid to the position of the towing point, which will influence the roll damping estimation result. Therefore, it is preferable to perform the roll decay tests with forward speed by free running models.

3.1.1 Model and installation

The model should be manufactured according to the ITTC Recommended Procedure 7.5-01-01-01, Ship Models, particular attention should be paid to model manufacturing tolerances, surface finish and appendage manufacture.

The model should be as large as possible for the size of the towing tank, taking into consideration wall blockage and finite depth effects (when performing the tests at forward speed).

All superstructures included in stability calculations or that may be submerged during the tests should be reproduced to ensure that the model has the correct righting arm curve.

The bilge keels or rudder, such as other relevant appendages, should be fitted to the hull model, properly scaled, and the report should state which appendages were fitted during the tests.

Following the guidelines from MSC.1/Circ. 1200 (IMO, 2006), to avoid scale effect on roll damping, the model overall length should be at least 4 m, unless frictional effect on roll damping is corrected with proper theoretical methods, but, in any case, not less than 2 m or a scale 1:75, whichever is greater. If the model is fitted with bilge keels, the model should be scaled up to make the breadth of the bilge keels greater than 7 mm.

The model should be ballasted to the appropriate displacement and the weights should be placed to achieve the correct position of the centre of gravity. Unsymmetrical weights distribution should be avoided, as far as practicable, in order to guarantee a reasonable radius of gyration for pitch.

Inclining tests should be carried out to verify that the ship's metacentric height $\overline{GM}$ corresponds to the desired one within an error of 2% or 1 mm at model scale, whichever is larger. In addition, roll radius of gyration in air (the preferred source) or natural roll period in water should be checked to correspond to the desired one within an error of 2%. To measure the natural roll period in water, roll decay tests should be performed but starting at a small roll amplitude (less than 5 deg), in order to avoid the influence of nonlinear effects due to the restoring and the damping moments. When measuring the oscillation angle of the model (for measuring the roll radius of gyration in air or the natural roll period in water), the same instrument that is used for the measurement of the roll motion should be used. The number of rolling period used for the estimation of the natural roll period should be, at least, 8.

When performing tests with no forward speed, the model should be placed in a transversal position with respect to the towing tank main direction and should be free, without any restriction, and the location should be to suffer the minimum wave reflection and distortion. If a (soft) restriction is used to restrain excessive drifting, it should be properly explained in the report document. The spring stiffness of the restraint lines should be based on the natural period consideration, i.e., the restraint system's natural period should be at least one order of magnitude greater than the model natural period.

When forward speed is considered and the ship model is towed, the position of the towing point is important, as for small angle of rolling, the roll axis is close to the waterplane and for large angle of rolling, the roll axis is close to the centre of gravity.

3.1.2 Measurement systems

The following quantities are measured:

- Roll motion, and motions in other degrees of freedom if necessary (simultaneously measured)
- Model speed (when performing free running tests with forward speed)
- Water temperature (for calculation of viscosity and density)

3.1.3 Instrumentation

<u>Model speed</u>

Refer to the ITTC Recommended Procedure 7.5-02-02-01, Resistance test.

<u>Temperature</u>

The water temperature should be measured at a depth near half of the model draught using a thermometer.

<u>Roll motion (and other degrees of freedom)</u>

The use of non-intrusive measurement systems to measure the ship motion is recommended, when feasible. If it is necessary to attach cables to the model, care should be taken to minimise interference.

The ship rotations and translations should be recorded at a sampling rate of, at least, 50 Hz sample rate.

The instrumentation installed on the model is considered as part of the ballast and needs to be in place when determining the centre of gravity and moments of inertia.

The location and orientation of the instrumentation should be documented.

3.1.4 Calibration

All devices used for data acquisition should be calibrated regularly. Calibration should generally be in accordance with ITTC Recommended Procedure 7.6-01-01 and following the advice of the manufacturer.

<u>Speed</u>

Refer to the ITTC Recommended Procedure 7.5-02-02-01, Resistance test.

<u>Thermometer</u>

Thermometer should be calibrated according to common standards and/or following the advice of the manufacturer and should be accurate to within 0.1ºC.

<u>Motion measurement system</u>

The motion measurement system used should be calibrated according to the advice of the manufacturer.

3.1.5 Pre-test considerations

Sign convention

Sign convention should be established for the basin, model and appropriate instrumentation, and should be documented adequately.

Following the model and instrumentation installation, and prior to perform the experiments, the sign convention of the instrumentation should be verified by applying a known translation or rotation to the ship model.

Calm water acquisition

Prior to perform the experiments, a data acquisition should be done in calm water of the ship position (and of the waves probes), to provide a record of "zero" levels. Additional calm water runs should be acquired throughout the experimental campaign, at the beginning of each day and after calibrating the instruments.

3.1.6 Test procedure and data acquisition

The data acquisition for each test should start before releasing the model, being the model at rest at the beginning of the recording. Then, the data acquisition should not be stopped until the model has reached rolling angles smaller than 0.5deg.

At least, 4 tests should be carried out where the initial angle should correspond to the largest initial heel angle that may be impressed to the ship model or, alternatively, the maximum angle of rolling amplitude that is of interest to estimate the roll damping. If the roll damping is very large or non-zero forward speed tests are carried out, the number of tests should be increased to obtain enough peaks of the roll angle.

During this test, no disturbance including wave propagating in the longitudinal direction of the basin and reflected by its end should be given to the model.

The procedure followed to heel initially the ship model should ensure that fulfilment of the initial conditions required in roll decay tests, i.e., zero angular velocity and no excitation to other degrees of freedom. To ensure these conditions and allow repeatability (reduce uncertainties), the initial heel angle should be impressed by using mechanical devices and reduce as far as possible human intervention.

For each test, recording of the roll time history should be saved and provided.

3.1.7 Data reduction and analysis

The speed of the test, when it exists, should be presented as a mean value derived from an integration of the instantaneous measured values over the same measuring interval.

Equivalent linear roll damping coefficient and nonlinear roll damping coefficients are calculated using the equations given in Section 2.

Analysis of model scale roll decay tests

Different methods to determine roll damping coefficients from roll decay tests exist. Most of them use the measured amplitude of the time history of rolling motion, as well as the instantaneous time where the amplitude occurs. Commonly used methods to analyse roll decay tests are (Haddara, 2005):

- *Logarithmic decrement method:* This method consists on determining the equivalent linear roll damping coefficient by assuming the linear differential equation defined by Eqs. (2) and (11), and then determine the nonlinear roll damping coefficients by least-squares fitting. The benefits of this methodology are that it may consider non-linearities in restoring and damping terms, it is simple and also allows to aggregate data from different decay tests (if they constitute the same test case) prior to perform the least-square fitting, which is more reliable than analysing each decay tests separately and calculating the mean of the determined non-linear damping coefficients. Further information of this method may be found in Appendix 1 of Bulian et al. (2009), Wassermann (2016a) and Oliveira et al. (2018)

- *Froude energy method:* This method equates the energy lost to damping in each half cycle to the work done by the restoring moment during the same period. Further information may be found in Froude (1955), Idle *et al.* (1912), Wassermann (2016a) and Oliveira et al. (2018)
- *Roberts energy method:* this method is based on the energy conservation, where the roll decrement is treated as an energy loss function, which is equated to the roll damping. Further information may be found in Roberts (1985) and Wassermann (2016a)
- *Least-squares iterative method:* this method constitutes a Parameter Identification Technique and is based on the fitting of the numerical solution of the nonlinear differential equation of roll to the time series of the decay test, performing an iterative fitting based on the least-squares method. Further information may be found in Section 4.6.2 of MSC. 1/Circ. 1200 and Oliveira et al. (2018). Using this technique does not presume a particular roll motion equation. Instead of the ordinary nonlinear differential equation, it can be used a full 6 DOF seakeeping tools, see Luthy et al. (2021).

3.2 Free running forced roll tests

Free running forced roll tests consist on exciting the ship to continuously roll applying an internal roll moment or regular beam waves, without any mechanic connection to the fixed world, i.e. with the ship free to move in all degrees of freedom.

3.2.1 Model and installation

Refer to section 3.1.1.

If a (soft) restriction is used to restrain excessive drifting, it should be properly explained in the report document. The spring stiffness of the restraint lines should be based on the natural period consideration, i.e., the restraint system's natural period should be at least one order of magnitude greater than the model natural period or the lowest wave period, when external regular waves are used.

3.2.2 Measurement systems

The following quantities are measured:

- Roll motion, and yaw and pitch if necessary (simultaneously measured)
- Rotating frequency and/or mass displacement of the mechanical system that impresses the transversal force (when applicable)
- Wave height (when applicable)
- Model speed (when considered)
- Water temperature (for calculation of viscosity and density)

3.2.3 Instrumentation

Apart from the information given in Section 3.1.3, the following instrumentation should be installed:

<u>Waves probes</u>

If the excitation is given by regular beam waves, wave height measurements should be made for all tests with wave probes fixed in the tank.

The wave probe position should be fixed to a position where disturbances from the motion of the model can be considered as negligible.

Roll moment generator (RMG)

If the excitation is given by internal devices, such as roll moment generators of gyroscopic type (the preferred way), contra-rotating masses etc., the actual rotating frequency or mass displacement should be measured.

3.2.4 Calibration

Apart from the information given in Section 3.1.4, the following aspects should be considered:

Wave calibration

When dealing with tests in bean regular waves, the wave generation quality should be assessed for the waves corresponding to the minimum and the maximum frequency used in the tests without the presence of the model, in order not to disturb the incident waves. When the measured double amplitude of the wave's elevation converges to a certain value, this value should be regarded as the wave height.

If tests are performed with forward speed, at least three waves probes should be positioned along the length of the basin and the variations in wave height and period should be within ± 5% among the different measured positions for the same wave.

External moment generator calibration

The external moment generators should be calibrated before performing the experiments in a range of rotating frequencies containing those tested for the model, with the model outside water and fixed.

For roll moment generators of gyroscopic types, the spin rate of each gyro should be calibrated, testing those spin rates that will be used in the forced roll experiments. Instead, the rotating frequency (tumbling frequency) to be checked could be limited to the natural frequency of the model.

Time histories of the generated moment during the calibrations should be saved and compared with numerical/analytical prediction, in order to disclose possible problems.

3.2.5 Pre-test considerations

Refer to Section 3.1.5.

3.2.6 Test procedure and data acquisition

The data acquisition for each run should start from calm water and the model at rest (about 20s), allowing an additional check on the performance of instrumentation and allowing to ensure that indication of zero drift is occurring. The acquisition should end after a sufficiently long steady state has been achieved, at least, if possible, 30 roll periods. However, in case of large interference due to reflected waves, recording of data could be stopped after about 15 roll periods after the first detection of disturbance.

The time windowing of the tests may be estimated by calculating the time required for the waves produced by the ship or the wave maker to come back after reflection from the towing tank side with an amplitude large enough to disturb the roll motion. As the wave front moves with a speed equal to the group speed, the time interval between the starting of the roll moment generator or the wave maker and the arrival of the direct wave front at the model position ΔT_{ref} $[s]$ can be estimated using the following formulation:

$$\begin{cases} \Delta T_{ref} = \frac{2 \cdot L_{ref}}{c_g} \\ c_g = \frac{1}{2} \cdot \frac{g}{2 \cdot \pi \cdot f_E} \end{cases} \tag{19}$$

where L_{ref} $[m]$ is the reference length and corresponds to the distance between the model and the reflecting wall under consideration, g $[m/s^2]$ is the acceleration of gravity, f_E $[Hz]$ is the frequency of motion or of the incident wave, c_g $[m/s]$ is the group speed according to a deep water assumption.

At least 9 frequencies should be tested for each loading condition and level of excitation (wave steepness). Given the (undamped) natural roll frequency ω_x , 7 standard frequencies should be checked:

$$\begin{bmatrix} 0.800, 0.900, 0.950, 0.975, \\ 1.000, 1.050, 1.200 \end{bmatrix} \cdot \omega_x$$

Two additional frequencies should be tested on the basis of a case-by-case analysis in order to have a good description of the roll response curve in the frequency region where the peak of the response curve is expected. More frequencies should be tested when a satisfactory description of the roll response curve cannot be achieved only by 9 frequencies.

When large rolling motions are expected, for ships with almost linear $\overline{GZ}$ in the range of tested roll angles, the peak should be found approximately at the natural frequencies. However, if this is not the case, care should be taken of the generally nonlinear softening behaviour of the restoring moment, as due to this behaviour, the peak of the response is usually found at a lower frequency than the natural frequency. On the other hand, for ships with S-shaped $\overline{GZ}$ curve, the peak could be found at a frequency higher than the natural one.

The level of excitation or wave steepness should be selected in order to meet from small to medium or large rolling amplitudes. It is important to define the small rolling amplitudes range to properly determine the linear damping coefficient μ. The maximum rolling amplitude determines the limit up to which the roll damping coefficients estimations are valid.

The time between each test and the following should be long enough to let the waves generated by the previous test dissipate.

For each test, the following data should be recorded:

- Time history of the roll angle
- Time history of the moment between the ship and the roll moment generator
- When using RMG of gyroscopic type, the time history of the rate of revolution of the main engine and the tumbling/rotating frequency and the measured value of the spin rates of the gyros

3.2.7 Data reduction and analysis

Equivalent linear roll damping coefficient and nonlinear roll damping coefficients are calculated using the equations given in Section 2.

<u>Analysis of free running forced roll tests</u>

Different methods to determine roll damping coefficients from free forced roll tests exist.

Most of them use the measured amplitude of the time history of rolling motion, as well as the instantaneous time where the amplitude occurs. Commonly used methods to analyse forced roll tests are (Haddara, 2005):

- *Quasi-linear method or Blume's method:* This method consists on determining the equivalent linear roll damping coefficient by assuming the linear differential equation defined by Eqs. (2) and (11), and then determine the nonlinear roll damping coefficients by least-squares fitting. In this method, the equivalent linear roll damping coefficient is determined from the ratio of the quasi-static heel angle and the measured dynamic roll amplitude, assuming that, at resonance, the inertial part and the restoring part of the equation of motion (approximately) cancel out, directly relating the amplitude of the forcing term at the peak response frequency with the damping term, as follows:

$$\begin{cases} \ddot{\varphi} + 2 \cdot \mu_{eq} \cdot \dot{\varphi} + \omega_x^2 \cdot \frac{\overline{GZ}(\varphi)}{\overline{GM}} = \\ \omega_x^2 \cdot \frac{K_a \cdot \sin(\omega_E \cdot t)}{\Delta \cdot \overline{GM}} \\ \varphi = \varphi_{res} \cdot \sin(\omega_{res} \cdot t) \end{cases} \quad (20)$$

At resonance:

$$2 \cdot \mu_{eq} \cdot \varphi_{res} \cdot \omega_{res} \approx \omega_x^2 \cdot \frac{K_a}{\Delta \cdot \overline{GM}} \Rightarrow$$

$$\Rightarrow \mu_{eq}(\varphi_{res}, \omega_{res}) \approx \frac{\omega_x^2 \cdot K_a}{2 \cdot \varphi_{res} \cdot \omega_{res} \cdot \Delta \cdot \overline{GM}}$$

where K_a $[N \cdot m]$ is the external transversal moment amplitude and φ_{res} $[\,rad\,]$ and ω_{res} $[rad/s]$ are the resonance peak amplitude and frequency, respectively.

Limitations of this method are the sole validity at the roll resonance frequency (Handschel et al., 2014a).

For further information, refer to Blume (1979), Wasserman et al. (2016a) and Oliva-Remola et al. (2018).

- *Energy method:* This method is based on equating the energy lost to damping in each cycle to the work done by the exciting moment. For further information, refer to Wasserman et al. (2016a).

- *Least-squares iterative method:* this method constitutes a Parameter Identification Technique and is based on the fitting of the numerical solution of the nonlinear differential equation of roll to the time series, performing an iterative fitting based on the least-squares method. When this methodology is used, at least two response curves obtained for two different wave steepness are strongly recommended to be used. Further information may be found in Section 4.6.2 of MSC. 1/Circ. 1200 (IMO, 2006)

3.3 (Semi-) Captive forced roll tests

Captive or semi-captive forced roll tests refer to ships being excited to continuously roll through an externally applied roll moment from an external oscillator between the towing carriage and the model. In this test, typically, a fixed roll axis is being prescribed during the forced roll motion. This circumstance simplifies the comparison of numerical simulations as it guarantees a pure roll motion and hence simplifies the analysis. However, since there is no “fixed roll axis” in a 6-DOF motion, this method should be applied with caution as the chosen position of the prescribed axis of rotation will influence the roll damping coefficients. In fact, for ensuring a correct roll motion at each time, especially the sway, pitch and heave motions shouldn’t be restrained during the forced roll motion tests. This leads to a more complex measuring/simulation and analysing technique, due to coupling contributions of different degrees of freedom.

As a result, it should be emphasized that the roll damping obtained from this type of tests is different from that of free running forced roll tests. The actual position of the roll axis must be included in the report.

3.3.1 Model and installation

Refer to section 3.1.1.

3.3.2 Measurement systems

The following quantities are measured:

- Model speed (when considered)
- Water temperature (for calculation of viscosity and density)
- Roll motion, and motions in other DoFs if necessary (simultaneously measured)
- Roll moment applied to the ship model

3.3.3 Instrumentation

Apart from the information given in Section 3.1.3, the following instrumentation should be installed:

<u>Mechanism to force the roll motion</u>

A mechanism to produce the rolling amplitudes about a virtual centre of roll should be installed. Preferably, the sway, pitch and heave motions shouldn't be restrained.

The choice for the position of the roll axis is extremely important. However, if the purpose of the tests is to validate CFD results, the position only needs to be the same as in the CFD.

<u>Strain gauges</u>

Strain gauges may be used to measure the roll moment experienced by the ship. Strain gauges should be placed at the locations where roll motions are generated.

The roll motion and roll moment must be measured simultaneously, because the phase angles are key elements to get the roll damping coefficients.

For further information, for partly-captured tests, refer to Hashimoto et al. (2009) and Grant et al. (2010). For examples of fully-captured tests, refer to Ikeda et al. (1976, 1977a, 1978a, 1990, 1994, 2000), Bassler et al. (2007), Katayama et al. (2008, 2009) and Handschel et al. (2014a).

3.3.4 Calibration

Apart from the information given in Section 3.1.4, the following aspects should be considered:

<u>Mechanism to force the roll motion</u>

The mechanism to force the roll motion should be calibrated before performing the experiments in a range of rotating frequencies containing those tested for the model.

Time histories of the generated motion during the calibrations should be saved and compared with numerical/analytical prediction, in order to disclose possible problems.

<u>Strain gauges</u>

Strain gauges should be calibrated according to the recommendations given by the manufacturer and following ITTC Recommended Procedure 7.6-01-01.

3.3.5 Pre-test considerations

Refer to Section 3.1.5.

3.3.6 Test procedure and data acquisition

The data acquisition for each run should start from calm water and the model at rest (about 20s), allowing an additional check on the performance of instrumentation and allowing to ensure that indication of zero drift is occurring. The acquisition should end after a sufficiently long steady state has been achieved, at least, if possible, 30 roll periods. However, in case of large interference due to reflected waves, recording of data could be stopped after about 15 roll periods after the first detection of disturbance.

If forced roll mechanism to generate the roll, the sampling rate needs to be high in order to accurately obtain the phase angle between roll motion and roll moment. The recommended value is 200Hz.

If regular waves are used to generate the roll, the time windowing of the tests may be estimated by calculating the time required for the waves produced by the ship or the wavemaker to come back after reflection from the towing tank side with an amplitude large enough to disturb the roll motion. As the wave front moves with a speed equal to the group speed, the time interval between the starting of the roll moment generator or the wavemaker and the arrival of the direct wave front at the model position ΔT_{ref} $[s]$ can be estimated using the following formulation:

$$\begin{cases} \Delta T_{ref} = \frac{2 \cdot L_{ref}}{c_g} \\ c_g = \frac{1}{2} \cdot \frac{g}{2 \cdot \pi \cdot f_E} \end{cases} \tag{21}$$

where L_{ref} $[m]$ is the reference length and corresponds to the distance between the model and the reflecting wall under consideration, g $[m/s^2]$ is the acceleration of gravity, f_E $[Hz]$ is the group speed according to a deep water assumption.

At least 9 frequencies should be tested for each loading condition and level of excitation (wave steepness). Given the (undamped) natural roll frequency ω_x , 7 standard frequencies should be checked:

$$\begin{bmatrix} 0.800, 0.900, 0.950, 0.975, \\ 1.000, 1.050, 1.200 \end{bmatrix} \cdot \omega_x$$

Two additional frequencies should be tested on the basis of a case-by-case analysis in order to have a good description of the roll response curve in the frequency region where the peak of the response curve is expected. More frequencies should be tested when a satisfactory description of the roll response curve cannot be achieved only by 9 frequencies.

When large rolling motions are expected, for ships with almost linear $\overline{GZ}$ in the range of tested roll angles, the peak should be found approximately at the natural frequencies. However, if this is not the case, care should be taken of the generally nonlinear softening behaviour of the restoring moment, as due to this behaviour, the peak of the response is usually found at a lower frequency than the natural frequency. On the other hand, for ships with S-shaped $\overline{GZ}$ curve, the peak could be found at a frequency higher than the natural one.

The rolling amplitudes tested should be selected in order to meet from small to medium or large rolling amplitudes. It is important to define the small rolling amplitudes range to properly determine the linear damping coefficient μ. The maximum rolling amplitude determines the limit up to which the roll damping coefficients estimations are valid.

The time between each test and the following should be long enough to let the waves generated by the previous test to dissipate.

For each test, the following data should be recorded:

- Time history of the forced roll angle
- Time history of the roll moment measured

3.3.7 Data reduction and analysis

Equivalent linear roll damping coefficient and nonlinear roll damping coefficients are calculated using the equations given in Section 2.

Analysis of (semi-) captive forced roll tests

Different methods to determine roll damping coefficients from (semi-) captive forced roll tests exist.

Most of them use the measured amplitude of the time history of rolling motion, as well as the instantaneous time where the amplitude occurs and the measured roll moment. Commonly used methods to analyse roll decay tests are (Handschel et al., 2014a):

- *Energy method:* This method is based on equating the energy lost to damping in each cycle to the work done by the exciting moment. For further information, refer to Handschel et al. (2014a).
- *Fourier transformation method:* this method consists on using a Fourier analysis to determine linear and non-linear components of the roll moment which are in phase with the roll velocity. For further information, refer to Handschel et al. (2014a).

3.4 General Comparison and Recommendations

A general comparison of the fore-mentioned test methods for roll damping measurement is given in Table 1.

To summarize, it is impossible to realize steady roll amplitude in free decay tests, while the forced roll tests can. The (semi-) captive forced roll tests can achieve the steadiest roll amplitudes and large roll amplitudes can be easily achieved, provided that the model is watertight. The free-running forced roll tests can also achieve steady roll amplitudes but the tested roll amplitudes depend on the capacity of roll motion generators (RMGs). It is possible to consider the forward speed effect on roll damping using all of the fore-mentioned test methods. However, it is difficult for free decay and free running forced roll tests because the free running setup are involved. For (semi-) captive forced roll tests, this presents no major difference compared with the zero speed tests.

Table 1 General Comparison

Item	Free decay	Free running forced roll	(Semi-) Captive forced roll
Steady roll ampl.	Impossible	Steady	Steadiest
Large roll ampl.	Temporarily	Depends on RMG	Easy to achieve
Forward speed effect	Possible	Possible but difficult	Possible and easy
Memory effect	Not fully included	Included	Included
CFD validation	Medium	Hard	Easy (1DoF Case)
Roll axis	Real/Time varying	Real/ Time varying	Prescribed/ Fixed
Time and cost	Cheap	Costly	Costly

Thanks to the steady periodic roll excitations, the forced roll tests can also take into account the memory effect of roll damping, which cannot be fully included in the free decay tests.

In terms of CFD validation purposes, the (semi-) captive forced roll tests are the easiest to validate because the roll motions are controlled, however, if motions in other DoFs are released, the difficulty of CFD validation increase tremendously. The free running forced roll tests are the hardest to validate, and free decay tests are in between.

Regarding time and cost, forced roll tests are costly because devoted test equipment or systems need to be developed. The free roll decay tests are cheap compared with forced roll tests.

4. PROCEDURE FOR ESTIMATING ROLL DAMPING FROM EMPIRICAL METHODS

This section describes the most used methods for roll damping estimation, which can be used in the absence of experimental data and can be used for dynamic stability calculations, such as the Ikeda's Method (Himeno, 1981) and the Simplified Ikeda's Method (Kawahara *et al.*, 2009).

It is important to note that, when considering the motion of a ship in waves, most of the hydrodynamic forces acting on a hull can be calculated using a potential theory. However, roll damping is significantly affected by viscous effects. Therefore, a result calculated using a potential theory overestimates the roll amplitude in resonance and is not accurate. It is common practice for the calculation of roll damping to use semi-empirical methods in order to consider the viscosity effects.

As stated in Section 2.4, when numerical computations are carried out using potential codes, caution should be taken not to double count the wave making component of roll damping.

4.1 Definition of Component Discrete Type Method

Most empirical methods are based on discretizing the roll damping in components. In a component discrete type method, the roll damping moment $B(\dot{\varphi})[N \cdot m]$ is predicted by summing up the predicted values of a number of components $B_{\varphi,i}$ $[N \cdot m]$. These components include the wave, lift, frictional, eddy and the appendages contributions (bilge keel, skeg, rudder, etc.):

$$B(\dot{\varphi}) = B_{\varphi,W} + B_{\varphi,L} + B_{\varphi,F} + B_{\varphi,E} + B_{\varphi,App} \tag{22}$$

The wave and lift components ($B_{\varphi,W}$ and $B_{\varphi,L}$) are linear components which are proportional to roll angular velocity $\dot{\varphi}$. The friction, eddy and appendage components ($B_{\varphi,F}$, $B_{\varphi,E}$ and $B_{\varphi,App}$) are nonlinear components.

If the nonlinear components are assumed to be proportional to $\dot{\varphi} \cdot |\dot{\varphi}|$, thus, if the linear-quadratic damping model is assumed (Eq. (8) or (9), fixing $B_{\varphi,3}$ or δ to zero), then, the equivalent linear roll damping coefficient B_{eq} (from now on called B_{44} $[(N \cdot m)/s]$) can be expressed as follows:

$$B_{44} = B_{44,W} + B_{44,L} + B_{44,F} + B_{44,E} + B_{44,App} \tag{23}$$

In the semi-empirical methods explained in Sections 4.2 and 4.3, the equivalent liner coefficient B_{44} is obtained following a linearization not explained in Section 2.4, due to its simplicity, which is based on equating the linearized damping moment to the non-linear one at the instant where the roll angular velocity takes its maximum value during steady oscillation. The linearization is as follows:

$$B_{44} = B_1 + \omega_E \cdot \varphi_a \cdot B_2 \tag{24}$$

Comparing Eq. (15) and Eq. (24), it may be seen that they differentiate by the term $8/(3 \cdot \pi)$, which leads to a difference of approximately 15% between the second terms of the right-hand sides of the equations. The latter form corresponds to a collocation method in a curve-fitting problem and it is not considered nowadays as valid for the analysis of roll motion. However, when the semi-empirical methods were developed, it was an extended formulation.

Taking as a basis the linearization of Eq. (24), the linearized roll damping moment is obtained by:

$$B_{44} = \frac{B(\dot{\varphi})}{\omega_E \cdot \varphi_a} \tag{25}$$

Then, following the approach followed by the semi-empirical methods of Sections 4.2 and 4.3, nonlinear components (i.e. $B_{\varphi,F}$, $B_{\varphi,E}$ and $B_{\varphi,App}$) are linearized using the linear-quadratic damping model of Eq. (15), as follows:

$$B_{44,E} = \frac{8}{3 \cdot \pi} \cdot (\omega_E \cdot \varphi_a) \cdot B_{\varphi,E} \tag{26}$$

It should be noted that all the coefficients in Eq. (22) and (23) depend on the roll frequency and the forward speed. The eddy and appendages components sometimes also depend on roll amplitude, because of the Keulegan-Carpenter number (K_e) effect in the vortex shedding problem.

The roll damping coefficient B_{44} $[(Nm)/s]$ is made non-dimensional as follows:

$$\hat{B}_{44} = \frac{B_{44}}{\rho \cdot \nabla \cdot B^2} \cdot \sqrt{\frac{B}{2 \cdot g}} \tag{27}$$

and the circular frequency of roll motion is also made non-dimensional as follows:

$$\widehat{\omega}_E = \omega_E \cdot \sqrt{\frac{B}{2 \cdot g}} \tag{28}$$

where ρ $[kg/m^3]$ is the mass density of water, ∇ $[m^3]$ is the ship displacement volume, B $[m]$ is the breadth of the ship's hull and g $[m/s^2]$ is the gravity acceleration.

The roll damping coefficient B_{44} can be translated into Bertin's N-coefficient $N(\varphi_a)$ (see Eq. (18)), assuming that the circular frequency of roll motion is equivalent to the (undamped) ship roll natural frequency:

$$\hat{B}_{44} = \frac{1}{\pi} \cdot \frac{\overline{GM} \cdot \varphi_a}{B \cdot \widehat{\omega}_E} \cdot N(\varphi_a) \tag{29}$$

where $\overline{GM}$ $[m]$ is the metacentric height with respect to the ship center of gravity, φ_a $[rad]$ is the steady rolling amplitude and B $[m]$ is the breadth of the ship's hull.

Please note that both φa and N-coefficient must be analyzed by using same units. For instance N-coefficient in Motora (1964) paper is analyzed by using [deg], in the case φa must be [deg] and 180 in place of π.

4.2 Ikeda's Method

In this section, the sectional roll damping coefficient is sometimes referred to the sectional roll damping coefficients are expressed with a prime on the right shoulder of a character (e.g. B'_{44E} $[N/s]$). For a 3-D ship hull form, the 3-D roll damping coefficient can be obtained by integrating the sectional roll damping coefficient over the ship length. Furthermore, a roll damping coefficient with subscript 0 (e.g. B'_{44E0} $[N/s]$) indicates a value at zero forward speed.

4.2.1 Displacement type mono-hull

<u>Wave making component</u>

The wave making component accounts for between 5% and 30% of the roll damping for a general-cargo type ship. However, the component may have a larger effect for ships with a shallow draught and wide section (Ikeda et al., 1978a).

In the case of zero Froude number, the wave damping can be easily obtained by using the strip method. It is however possible to numerically solve the exact wave problem for a 3-D ship hull form. Using the strip method, the sectional wave damping is calculated from the solution of a sectional wave problem, taking the form:

$$B'_{44\mathrm{W0}} = B'_{22}\left(l_{\mathrm{w}} - \overline{OG}\right)^2 \quad (30)$$

where B'_{22} and l_w represent the sectional sway damping coefficient and the moment lever measured from the still water level due to the sway damping force(for example, if the wave damping component is calculated using a strip method based on potential theory, B'_{22} and B'_{42}, which are sectional damping values caused by sway, are obtained from the calculation, and l_w is obtained from B'_{42} divided by B'_{22}.). $\overline{OG}$ represents the distance from the still water level O to the roll axis G with positive being downward.

With non-zero forward ship speed, it is difficult to treat the wave roll damping theoretica1y.However, there are methods that can be used as approximate treatments for predicting the wave damping at forward speed. The first is the method in which the flow field due to roll motion is expressed by oscillating dipoles with horizontal lateral axes. The roll damping is then obtained approximately from the wave-energy loss in the far field. Ikeda *et al.*, (1978a) calculated the energy loss in the far field due to a pair of horizontal doublets and compared the results with experiments for models of combined flat plates. From this elementary analysis, they proposed an empirical formula for roll damping of typical ship forms (Ikeda *et al.*, 1978a):

$$\frac{B_{44W}}{B_{44\mathrm{W0}}} = 0.5 \cdot \begin{bmatrix} (A_2+1) + \\ (A_2-1)\cdot\tanh(20\cdot\Omega-0.3) + \\ (2A_1-A_2-1)\cdot \\ \quad \exp\{-150\cdot(\Omega-0.25)^2\} \end{bmatrix} \quad (31)$$

where:

$$A_1 = 1 + \xi_{\mathrm{d}}^{-1.2} e^{-2\xi_{\mathrm{d}}}$$
$$A_2 = 0.5 + \xi_{\mathrm{d}}^{-1} e^{-2\xi_{\mathrm{d}}} \quad (32)$$
$$\xi_{\mathrm{d}} = \frac{\omega_{\mathrm{E}}^2 d}{g}\ ;\ \Omega = \frac{V\omega_{\mathrm{E}}}{g}$$

$B_{44\mathrm{W0}}$ represents the wave damping at zero forward speed which can be obtained by a strip method. V and d are forward velocity and draught of hull. However, it appears that there are still some difficulties to be considered with this method. There is a limitation in application to certain ship forms, particularly in the case of small draught-beam ratios (Ikeda *et al.*, 1978a).

<u>Hull lift component</u>

Since the lift force acts on the ship hull moving forward with sway motion, it can therefore be concluded that a lift effect occurs for ships during roll motion as well. The prediction formula for this component is as follows (Ikeda *et al.*, 1978a, 1978b):

$$B_{44,\mathrm{L}} = \frac{\rho}{2}\cdot V\cdot L\cdot d\cdot k_{\mathrm{N}}\cdot l_0\cdot l_{\mathrm{R}}\cdot \cdot\left[1.0 - 1.4\cdot\frac{\overline{OG}}{l_{\mathrm{R}}} + \frac{0.7\cdot\overline{OG}^2}{l_0\cdot l_{\mathrm{R}}}\right] \quad (33)$$

where

$$l_0 = 0.3\cdot d \quad ; \quad l_{\mathrm{R}} = 0.5\cdot d \quad (34)$$

$$k_{\mathrm{N}} = 2\cdot\pi\cdot\frac{d}{L} + \kappa\cdot\left(4.1\cdot\frac{B}{L} - 0.045\right) \quad (35)$$

$$\kappa = \begin{cases} 0.0 & C_m \le 0.92 \\ 0.1 \quad for & 0.92 < C_m \le 0.97 \\ 0.3 & 0.97 < C_m \end{cases} \quad (36)$$

where $C_M = A_M/(B\,d)$ (C_M: midship section coefficients, A_M: area of midship section).

In Eq.(33), k_N represents the lift slope often used in the field of ship manoeuvring. The lever l_0 is defined in such a way that the quantity $l_0\cdot\dot{\varphi}/V$ corresponds to the angle of attack of the lifting body. The other lever l_R denotes the distance from the point O (the still water level) to the centre of lift force.

<u>Frictional component</u>

The frictional component accounts for between 8% and 10% of the total roll damping for a 2m long model ship (Ikeda et al., 1976, 1978a). However, this component is influenced by Reynolds number (scale effects), and so the proportion decreases in proportion to ship size and only accounts for between 1% and 3% for full scale ships. Other components of the roll damping do not have such scale effects. Therefore, even if the scale of a ship is varied, the same non-dimensional damping coefficient can be used for the other components excluding the frictional component.

Kato (1957) deduced a semi-empirical formula for the frictional component of the roll damping from experimental results on circular cylinders completely immersed in water. It was found that the frictional damping for rolling cylinders can be expressed in the same form as that given by Blasius (1908, 1950) for laminar flow, when the effective Reynolds number is defined as:

$$Re = \frac{0.512\ r^2\, \varphi_{\mathrm{a}}^2\, \omega_{\mathrm{E}}}{\nu} \tag{37}$$

where r is radius of cylinder, ν is kinematic viscosity. The frictional coefficient C_{f} is defined (Hughes, 1954) as:

$$C_{\mathrm{f}} = 1.328\left(\frac{3.22\ r_{\mathrm{f}}^2\, \varphi_{\mathrm{a}}^2}{T_{\mathrm{R}}\nu}\right)^{-0.5} \tag{38}$$

The damping coefficient due to surface friction for laminar flow in the case of zero ship speed can be represented as:

$$B'_{44\mathrm{F0}} = \frac{4}{3\pi}\rho\, S_{\mathrm{f}}\, r_{\mathrm{f}}^3\, \varphi_{\mathrm{a}}\, \omega_{\mathrm{E}} C_{\mathrm{f}} \tag{39}$$

where the value of S_{f} and r_{f} for a 3-D ship hull form can be estimated by following regression formulas (Kato, 1957):

$$S_{\mathrm{f}} = L_{pp}\,(1.7d + C_{\mathrm{B}}B) \tag{40}$$

$$r_{\mathrm{f}} = \frac{1}{\pi}\left\{ \begin{matrix} (0.887 + 0.145\, C_{\mathrm{B}})\ (1.7d + C_{\mathrm{B}}B) - \\ 2\overline{OG} \end{matrix} \right\} \tag{39.1}$$

This component increases slightly with forward speed, and so a semi-theoretical method to modify the coefficient in order to account for the effect of the forward speed on the friction component was proposed by Tamiya et al, (1972). The combination of Kato and Tamiya's formulae is found to be accurate for practical use and is expressed as:

$$B_{44\mathrm{F}} = B_{44\mathrm{F0}}\left(1 + 4.1\frac{V}{\omega_{\mathrm{E}}\, L}\right) \tag{41}$$

where $B_{44\mathrm{F0}}$ is the 3-D damping coefficient which can be obtained by integrating the sectional damping coefficient $B'_{44\mathrm{F0}}$ in Eq.(39) over the ship length.

The applicability of this formula has also been confirmed through Ikeda's analysis (Ikeda et al, 1976) on the 3-D turbulent boundary layer over the hull of an oscillating ellipsoid in roll motion.

<u>Eddy making component</u>

At zero forward speed, the eddy making component for a naked hull is mainly due to the sectional vortices. Fig. 1 schematically shows the location of the eddies generated around the ship hull during the roll motion (Ikeda *et al.*,(1977a),(1978b)). The number of eddies generated depends on two parameters relating to the hull shape, which are the half breadth-draught ratio H_0 ($=B/2d$) and the area coefficient σ ($=A_{\mathrm{j}}/Bd$, A_{j}: the area of the cross section under water).

Ikeda *et al*, (1978a) found from experiments on a number of two-dimensional cylinders with various sections that this component for a naked hull is proportional to the square of both the roll frequency and the roll amplitude. In other words, the coefficient does not depend on *Ke* number, but the hull form only:

$$C_R = \frac{M_{\phi E}}{\frac{1}{2}\rho\, d^4 L\ \dot{\varphi}\ |\dot{\varphi}|} \tag{42}$$

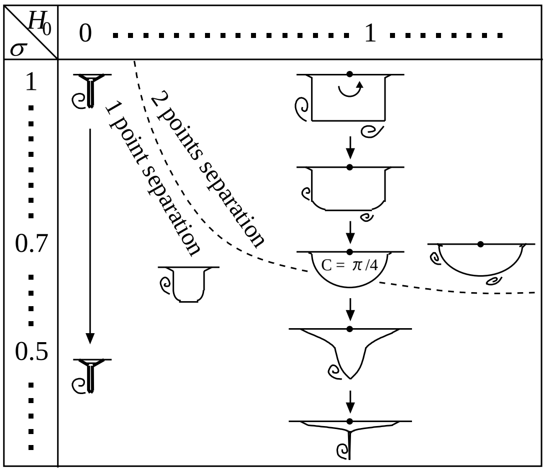

Fig. 1 Vortices shed from hull (Ikeda et al., 1977a).

A simple form for the pressure distribution on the hull surface as shown in Fig. 2 can be used.

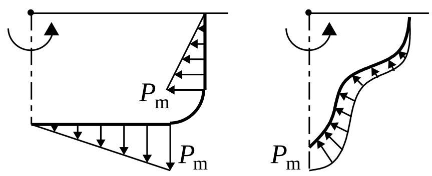

Fig. 2 Assumed profile of pressure distribution (Ikeda et al., 1977a).

The magnitude of the pressure coefficient C_p can be taken as a function of the ratio of the maximum relative velocity to the mean velocity on the hull surface $\gamma = V_{max}/V_{mean}$. This can be calculated approximately by using the potential flow theory for a rotating Lewis-form cylinder in an infinite fluid. The C_p-γ curve is thus obtained from the experimental results of the roll damping for 2-D models.

The eddy making component at zero forward speed can be expressed by fitting this pressure coefficient C_p with an approximate function of γ, by the following formula (Ikeda *et al*, 1977a, 1978a, Katayama *et al.*, 2022):

$$B'_{44E0} = \frac{4\ \rho\, d^4 \omega_E \varphi_a}{3\pi} C_R \tag{43}$$

$$C_R = \left\{\left(1 - f_1\ \frac{R}{d}\right)\left(1 - \frac{3}{2}\frac{\overline{OG}}{d} - f_1\frac{R}{d}\right) + \right.$$
$$\left. + f_2\ \left(H_0 - f_1\ \frac{R}{d}\right)^2\right\} \cdot C_p\left(\frac{r_{max}}{d}\right)^2$$

$$C_p = 0.5\ \left(0.87e^{-\gamma} - 4e^{-0.187\gamma} + 3\right)$$

where:

$$f_1 = 0.5\ \left[1 + tanh\{\,20\ (\sigma - 0.7)\}\right]$$

$$f_2 = 0.5(1 - cos\pi\sigma) -$$
$$-1.5\left(1 - e^{-5(1-\sigma)}\right)\sin^2\pi\sigma$$

and the value of γ is obtained as follows:

$$\gamma = \frac{\sqrt{\pi} f_3\left(r_{\max} + \frac{2M}{H}\right)\ \sqrt{A^2 + B^2}}{2d\ \left(1 - \frac{\overline{OG}}{d}\right)\ \sqrt{H_0'\sigma'}} \tag{44}$$

$$M = \frac{B}{2\ (1 + a_1 + a_3)}$$

$$H_0' = \frac{H_0}{1 - \overline{OG}/d}$$

$$\sigma' = \frac{\sigma - \overline{OG}/d}{1 - \overline{OG}/d}$$

$$H = 1 + a_1^2 + 9\ a_3^2 + 2\ a_1(1 - 3a_3)\ cos2\ \psi - 6\ a_3 cos4\ \psi$$

$$A_0 = -2\ a_3\ cos5\ \psi + a_1(1 - a_3)\ cos3\ \psi + \{(6 - 3a_1)\ a_3^2 + (a_1^2 - 3a_1)\ a_3 + a_1^2\}cos\ \psi$$

$$B_0 = -2\ a_3\ sin5\ \psi + a_1(1-a_3)\ sin3\ \psi + \{(6+3a_1)\ a_3^2 + (3a_1 + a_1^2)\ a_3 + a_1^2\} sin\ \psi$$

$$r_{max} = M\sqrt{\{(1+a_1)\ sin\ \psi - a_3 sin3\psi\}^2 + \{(1-a_1)\ cos\ \psi + a_3 cos3\psi\}^2}$$

where a_1, a_3 are the Lewis-form parameters. ψ represents the Lewis argument on the transformed unit circle. Values ψ and f_3 are (Katayama *et al*. 2022):

$$\psi = \begin{cases}\psi_1 & (r_{max}(\psi_1) \geq r_{max}(\psi_2)) \\ \psi_2 & (r_{max}(\psi_1) < r_{max}(\psi_2))\end{cases}$$

$$\psi_1 = 0$$

$$\psi_2 = \begin{cases}\frac{1}{2}\cos^{-1}\frac{a_1(1+a_3)}{4a_3} & \left(\left|\frac{a_1(1+a_3)}{4a_3}\right| \leq 1\right) \\ \tan^{-1} H_0 & \left(\left|\frac{a_1(1+a_3)}{4a_3}\right| > 1\right)\end{cases}$$

$$f_3 = 1 + 4exp\{-1.65 \times 10^5(1-\sigma)^2\}$$

For a 3-D ship hull form, the eddy making component is given by integrating B_{E0} over the ship length.

This component decreases rapidly with forward speed and reduces to a non-linear correction for the (linear) lift force on a ship, or wing, with a small angle of attack. From experimental results for ship models a formula for this component at forward speed can be determined empirically as follows (Ikeda *et al*, 1978a):

$$B_{44\mathrm{E}} = B_{44\mathrm{E0}}\frac{(0.04K)^2}{1+(0.04K)^2} \tag{45}$$

where K is the reduced frequency ($=\omega L/U$).

The above-mentioned Eq.(43) applies to a sharp-cornered box hull with normal breadth-draught ratio, but not to a very shallow draught. Yamashita *et al*, (1980) confirmed that the method gives a good result for a very flat ship when the roll axis is located at the water surface. Standing (1991), however, pointed out that Eq.(43) underestimates the roll damping of a barge model. To confirm the contradictions, Ikeda *et al*, (1993) carried out an experimental study on the roll damping of a very flat barge model and proposed a simplified formula for predicting the eddy component of the roll damping of the barge as follows (Ikeda *et al*, 1993):

$$B'_{44\mathrm{E0}} = \frac{2}{\pi}\rho L d^4\left(H_0^2 + 1 - \frac{3}{2}\frac{\overline{OG}}{d}\right) \times \left\{H_0^2 + \left(1 - \frac{\overline{OG}}{d}\right)^2\right\}\varphi_{\mathrm{a}}\omega_{\mathrm{E}} \tag{46}$$

<u>Appendages component</u>

Bilge keel component

The bilge keel component $B_{44\mathrm{BK}}$ is divided into four components:

$$B_{44\mathrm{BK}} = B_{44\mathrm{BKN0}} + B_{44\mathrm{BKH0}} + B_{44\mathrm{BKL}} + B_{44\mathrm{BKW}} \tag{47}$$

For the case of large amplitude roll motion, where the bilge keel may be above water surface at the moment of maximum roll angle, Bassler *et al*, (2010) proposed as a piecewise function of roll angle for the B_{44BK} component.

The normal force component $B_{44\mathrm{BKN0}}$ can be deduced from the experimental results of oscillating flat plates (Ikeda *et al*, 1978c, 1978d).The drag coefficient C_D of an oscillating flat plate depends on the Ke number. From the measurement of the drag coefficient, C_D, from free roll tests of an ellipsoid with and without bilge keels, the prediction formula for the drag coefficient of the normal force of a pair of the bilge keels can be expressed as follows:

$$C_D = 22.5\frac{b_{\mathrm{BK}}}{\pi\ l\varphi_{\mathrm{a}}f} + 2.4 \tag{48}$$

where b_{BK} is the breadth of the bilge keel and l is the distance from the roll axis to the point on hull with bilge keel attached. Wassermann *et al*(2016b) extended the above equation for Ke ranging from 0.3 < Ke < 20.

$$C_D = 0.7 \cdot \ln(Ke)^2 - 4.94 \cdot \ln(Ke) + 13.75 \tag{49}$$

Further simulations for 20 < Ke < 100 where performed which are taking into account by the above equation as well but are not validated by experiments.

The equivalent linear damping coefficient B'_{44BKN0} is:

$$B'_{44\mathrm{BKN0}} = \frac{8}{3\pi}\rho\ l^3\omega_{\mathrm{E}}\varphi_{\mathrm{a}}b_{\mathrm{BK}}f^2\ C_D \tag{50}$$

where f is a correction factor to take account of the increment of flow velocity at the bilge, determined from the experiments:

$$f = 1 + 0.3e^{\{-160(1-\sigma)\}} \tag{51}$$

From the measurement of the pressure on the hull surface caused by the bilge keels, it was found that the coefficient C_p^+ of pressure on the front face of the bilge keels does not depend on the Ke number. However, the coefficient C_p of the pressure on the back face of bilge keel and the length of negative-pressure region do depend on the Ke number. From these results, the length of the negative-pressure region can be obtained as follows:

$$S_0/b_{\mathrm{BK}} = 0.3\frac{\pi\ l\varphi_{\mathrm{a}}f}{b_{\mathrm{BK}}} + 1.95 \tag{52}$$

assuming a pressure distribution on the hull as shown in Fig. 3.

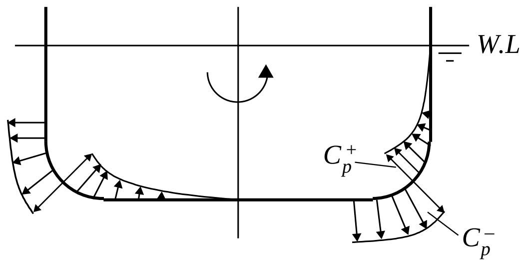

Fig. 3 Assumed pressure distribution on the hull surface caused by bilge keels (Ikeda et al., 1976).

The roll damping coefficient B'_{BKH0} can be expressed as follows (Ikeda *et al*, 1978c, 1978d):

$$B'_{44\mathrm{BKH0}} = \frac{4}{3\pi}\rho\ l^2f^2\omega_{\mathrm{E}}\varphi_{\mathrm{a}}\int_G C_p \cdot l_{\mathrm{p}}\, dG \tag{53}$$

where G is length along the girth and l_p is the moment lever.

The coefficient C_p^+ can be taken approximately as 1.2 empirically. From the relation of $C_D = C_p^+ - C_p^-$, the coefficient C_p^- can be obtained as follows:

$$C_p^- = 1.2 - C_D = -22.5\frac{b_{\mathrm{BK}}}{\pi\ l\varphi_{\mathrm{a}}f} - 1.2 \tag{54}$$

The value of $\int_G C_p \cdot l_{\mathrm{p}}\, dG$ in Eq.(53) can be obtained as follows:

$$\int_G C_p \cdot l_{\mathrm{p}}\ dG = d^2\left(-A_0C_p^- + B_0C_p^+\right) \tag{55}$$

where:

$$A_0 = (m_3 + m_4)m_8 - m_7^2$$

$$B_0 = \frac{m_4^3}{3(H_0 - 0.215m_1)} + \frac{(1-m_1)^2(2m_3 - m_2)}{6(1-0.215m_1)} + m_1(m_3m_5 + m_4m_6)$$

$$m_1 = R/d$$
$$m_2 = \overline{OG}/d$$
$$m_3 = 1 - m_1 - m_2$$
$$m_4 = H_0 - m_1$$

$$m_5=\frac{\begin{Bmatrix}0.414H_0+0.0651m_1^2- \\ \quad (0.382H_0+0.0106)m_1\end{Bmatrix}}{(H_0-0.215m_1)(1-0.215m_1)}$$

$$m_6=\frac{\begin{Bmatrix}0.414H_0+0.0651m_1^2- \\ \quad (0.382+0.0106H_0)m_1\end{Bmatrix}}{(H_0-0.215m_1)(1-0.215m_1)}$$

$$m_7=\begin{cases}S_0/d-0.25\pi\, m_1, & S_0>0.25\pi\, R\\ 0\qquad\qquad\quad , & S_0\le 0.25\pi R\end{cases}$$

$$m_8=\begin{cases}m_7+0.414m_1 & , \ S_0>0.25\pi R\\ m_7+1.414m_1\left(1-cos(\frac{S_0}{R})\right), & S_0\le 0.25\pi R\end{cases}$$

where l is distance from roll axis to the tip of bilge keels and R is the bilge radius. These are calculated as follows:

$$l=d\sqrt{\begin{array}{l}\left\{H_0-\left(1-\frac{\sqrt{2}}{2}\right)\frac{R}{d}\right\}^2+\\ \qquad\left\{1-\frac{\overline{OG}}{d}-\left(1-\frac{\sqrt{2}}{2}\right)\frac{R}{d}\right\}^2\end{array}} \tag{56}$$

$$R=\begin{cases}2d\sqrt{\frac{H_0(\sigma-1)}{\pi-4}}\ , & R<d \ \ \& \ \ R<\frac{B}{2}\\ d\ , & H_0\ge 1 \ \ \& \ \ \frac{R}{d}>1\\ \frac{B}{2}\ , & H_0\le 1 \ \ \& \ \ \frac{R}{d}>H_0\end{cases} \tag{57}$$

To predict the bilge keel component, the prediction method assumes that a cross section consists of a vertical side wall, a horizontal bottom and a bilge radius of a quarter circle for simplicity. The location and angle of the bilge keel are taken to be the middle point of the arc of the quarter circle and perpendicular to the hull surface. It may not be possible to satisfactorily apply these assumptions to the real cross section if it has large differences from a conventional hull with small bilge radius as shown in

Fig. 4 for a high-speed slender vessel (Ikeda *et al*, 1994).

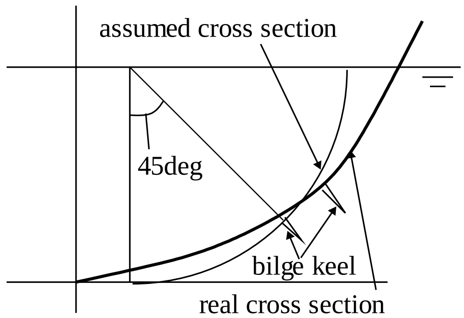

Fig. 4 Comparison between cross section, fitting position and the angle of bilge keel assumed in prediction method and those of high-speed slender vessels (Ikeda et al, 1994).

These assumptions cause some element of error in the calculation of the moment levers of the normal force of the bilge keels and of the pressure force distributed on the hull surface caused by the bilge keel. In such a case, Eq.(55) should be calculated directly. The pressure distribution can be taken as shown in Fig. 3and the length of negative pressure C_p^-can be defined by using parameter B in Eq.(55).

In the estimation method, it is assumed that the effect of forward speed on the bilge keel component is small and can be ignored. However, it is hard to ignore the lift force acting on the bilge keel if a vessel has high forward speed. Since a bilge keel can be regarded as a small aspect ratio wing, Jones's theory can be applied to it where the flow is composed of forward speed $V=Fr\sqrt{gL}$ and the tangential velocity caused by roll motion $u=l_1\dot{\phi}=l_1\phi_{\mathrm{a}}\omega_{\mathrm{E}}$ (where l_1 denotes the distance between the centre of roll axis and the centre of bilge keel)the attack angle and the resultant flow velocity are obtained as$\alpha=\tan^{-1}(u/V)$ and $V_R=\sqrt{V^2+u^2}$ respectively. On the basis of Jones's theory, the lift force acting on a bilge keel is expressed as (Ikeda *et al*, 1994):

$$L_{\mathrm{BK}} = \frac{\pi\rho\alpha {V_R}^2 {b_{\mathrm{BK}}}^2}{2} \tag{58}$$

where b_{BK} is the maximum breadth of the bilge keel. The roll damping coefficient due to a pair of bilge keels $B_{44\mathrm{BKL}}$ can be obtained as follows:

$$B_{44\mathrm{BKL}} = \frac{2\ L_{\mathrm{BK}}\ l_1}{\varphi_{\mathrm{a}}\ \omega_{\mathrm{E}}} \tag{59}$$

The wave making contribution from the bilge keels at zero forward speed$B_{44\mathrm{BKW0}}$ is expressed as (Bassler *et al*, 2009):

$$\hat{B}_{44\mathrm{BKW0}} \sim C_{\mathrm{BK}}(b_{\mathrm{BK}})\exp\left(-\frac{\omega^2}{g} d_{\mathrm{BK}}(\varphi)\right) \tag{60}$$

where the source strength C_{BK} is a function of the bilge keel breadth b_{BK}. In this equation, the bilge keel may be considered as a source, pulsing at frequency ω_e at a depth relative to the free surface, d_{BK} in Fig. 5, based on the roll amplitude. For simplicity, C_{BK} is assumed to be the ratio of the bilge keel breadth to ship beam. The damping is assumed to be zero for zero roll amplitude. The distance from the free surface to the bilge keel, d_{BK}, is given by:

$$d_{\mathrm{BK}}(\varphi) = l_{\mathrm{BK}}\begin{bmatrix}\left(\frac{(2d/B)}{\sqrt{1+(2d/B)^2}}\right)\ \cos\varphi - \\ \sin\varphi\ \left(\frac{1}{\sqrt{1+(2d/B)^2}}\right)\end{bmatrix} \tag{61}$$

where d is the draught, B is the beam, and ϕ is the roll angle, Fig. 5. The effects of forward speed are taken into account by Eq.$B44WB44W0 = 0.5 \cdot \begin{bmatrix} (A_2+1) + \\ (A_2-1)\cdot\tanh(20\cdot\Omega-0.3) + \\ (2A_1-A_2-1)\cdot \\ \exp\{-150\cdot(\Omega-0.25)^2\}\end{bmatrix}$ (31).

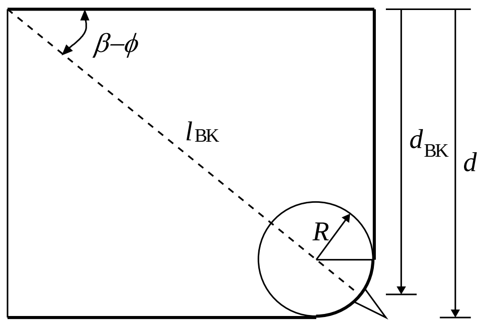

Fig. 5 Illustration of the bilge keel depth, d_{BK}, as a function of roll angle, ϕ; and distance from the roll axis to the bilge keel, l_{BK}, for the half-midship section of a conventional hull form.(Bassler *et al*, 2009)

Skeg component

The skeg component of the roll damping is obtained by integrating the assumed pressure caused by the skeg, as shown in Fig. 6 over the skeg and the hull surface.

The skeg component of the roll damping per unit length can be expressed as follows (Ali et al., 2004):

$$B'_{44\mathrm{SK0}} = \frac{4}{3\pi}\varphi_{\mathrm{a}} l^2 \omega_{\mathrm{E}}\rho\begin{pmatrix} C_D l_{\mathrm{SK}} l_1 - \\ 0.5 C_p^+ a l_2 + \\ \frac{3}{4} C_p^- S l_3 \end{pmatrix} \tag{62}$$

$$C_D = (C_p^+ - C_p^-) = C_{D0} e^{\left(\frac{-0.38 b_{SK}}{l_{SK}}\right)}$$

$$C_p^+ = 1.2$$

$$C_{D0} = \begin{cases} 2.425Ke\ , & 0 \le Ke \le 2 \\ -0.3Ke + 5.45, & Ke > 2 \end{cases}$$

$$Ke = \frac{U_{max} T_e}{2 l_{SK}} = \frac{\pi \varphi_a l}{l_{SK}}$$

$$S = 1.65 Ke^{2/3} \cdot l_{SK}$$

where C_p^+, $C_p^-$and l_2, l_3 denote representative pressure coefficients and their moment levers obtained by integrating the pressure distribution on the hull surface in front of and on the back face of the skeg respectively. l is the distance from the axis of roll rotation to the tip of the skeg. l_{SK} and b_{SK} are the height and thickness of skeg respectively, Ke is the Keulegan-Carpenter number for the skeg, U_{max} is the maximum tangential speed of the edge of the skeg, T_e is the period of roll motion and S is the distribution length of negative pressure on hull surface caused by the skeg.

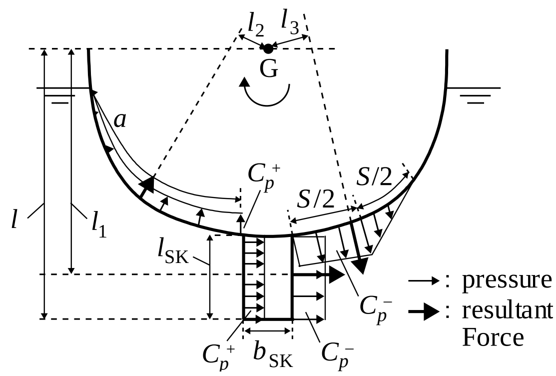

Fig. 6 Assumed pressure caused by a skeg (Ali et al., 2004).

4.2.2 Hard chine type hull

Generally, the roll damping acting on a cross section can be divided into a frictional component, a wave making component, an eddy making component, a bilge-keel component and a skeg component. Bilge keel and skeg components are caused by separated vortices. However, it is more convenient practically to treat them as independent components, without including them in the eddy making component. Although the friction component may be around 10% of the roll damping from measured model data (model length under approximate 4m, refer to IMO MSC.1/ Circ.1200 ANNEX, Page 7, 4.3.2), it is only up to approximately 3% for a full-scale vessel. This means therefore, that the friction component can be effectively ignored. The wave making component can again be treated using the theoretical calculation based on potential theory as defined previously for displacement hulls. Therefore, it is recommended to also apply these calculation methods to hard chine type hulls.

<u>Eddy making component</u>

The eddy making component of a hard chine type hull is mainly caused by the separated vortices from the chine. The sectional pressure distribution on hull caused by this separated vortex is approximated by a simple formulation and the roll damping is calculated by integrating it along the hull surface.

The length and the value of the pressure distribution are decided upon based on the measured pressure and the measured roll damping. Initially, the estimation method is used for the case where the rise of floor is 0. The pressure distribution is assumed to like that shown in Fig. 7.

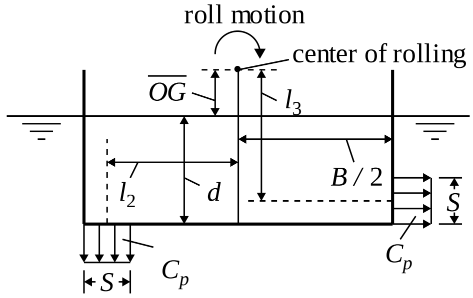

Fig. 7 Assumed pressure distribution caused by separated flow from hard chine(Ikeda et al, 1990).

The sectional roll damping coefficient is calculated from the following:

$$B'_{44E0} = \frac{4}{3\pi}\rho\varphi_a\omega_E C_p\ S\ (l_2 + l_3)l^2 \tag{63}$$

where, l_2 and l_3 are the moment levers shown in Fig. 7, and l is the distance from the axis of roll rotation to the chine (Ikeda et al, 1990).

The length of the negative pressure S and its pressure coefficient C_p are expressed as the function $H_0{*}\left(= B/\left(2d - 2\overline{OG}\right)\right)$. These are obtained from the following equations based on measured data:

$$S = (0.3H_0 * -0.1775 + \frac{0.0775}{H_0*^2})d \tag{64}$$

$$C_p = \exp(k_1 H_0 * + k_2) \tag{65}$$

where:

$$k_1 = -\exp\begin{pmatrix}-0.114H_0{}^2 + \\ 0.584H_0 - 0.558\end{pmatrix}$$
$$k_2 = -0.38H_0{}^2 + 2.264H_0 + 0.748 \tag{66}$$

When there is a rise of floor, the moment lever not only changes, but the length of the negative pressure distribution and its pressure coefficient also change. However, the effect of the rise of floor on the size of a separated vortex is not well understood. Therefore, the effect of rise of floor is taken into consideration by modifying the coefficient as a function of the rise of floor. S and C_p are multiplied by the following empirical modification coefficient (Ikeda *et al*, 1990):

$$f_1(\alpha) = \exp(-2.145\beta) \tag{67}$$

$$f_2(\alpha) = \exp(-1.718\beta) \tag{68}$$

Using the above method, the eddy making component of a cross section can be estimated. The depth of the chine d_c, the half breadth to draught ratio H_0 (=$B/2d$) of a cross section, draught d, rise of floor β, and vertical distance from water surface to the centre of gravity (axis of roll rotation) $\overline{OG}$ (downward positive) are required for the estimation.

<u>Skeg component</u>

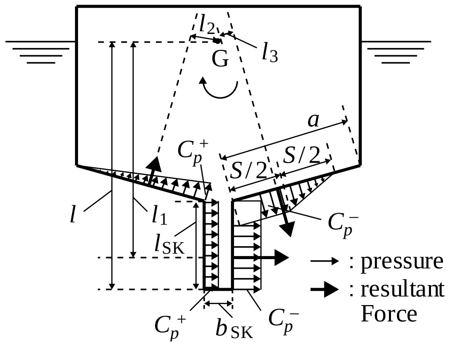

Fig. 8 Assumed pressure distribution caused by skeg (Tanaka et al., 1985).

An estimation method for the skeg component has been proposed by Tanaka *et al*, (1985). Using this method, the shape of the approximated pressure distribution is shown in Fig. 8.

From the integration of the pressure distribution, the roll damping coefficient for the cross section is expressed by the following:

$$B'_{44SK0} = \frac{8}{3\pi}\rho\ \varphi_a l^2\omega_E \begin{Bmatrix} C_D l_{SK} l_1 - \\ 0.5C_p^+ a l_2 + \\ \frac{3}{4}C_p^- S l_3 \end{Bmatrix} \tag{69}$$

$$C_D = C_p^+ - C_p^-$$
$$C_p^- = -3.8$$
$$C_p^+ = 1.2$$
$$S = 1.65Ke^{\frac{2}{3}} l_{SK}$$
$$Ke = U_{max}\frac{T_e}{2l_{SK}}$$

Here, U_{max} is the maximum tangential speed at the centre of skeg, T_e is roll period, l_{SK}, b_{SK} are the height and thickness of skeg, and l is the distance from the axis of roll rotation to the tip of the skeg. In this estimation method, the skeg is assumed to be a flat plate and the pressure coefficient is assumed to be constant based on the measured results from an oscillated flat plate with a flat plate skeg (Tanaka *et al*, 1985). However, an Asian coastal fishing boat may have a wide breadth due to the stability requirements for the boat and due to the strength of the skeg required in service (Ikeda *et al*, 1990). In this case, not only should the measured results from a flat plate be considered, but also the measured results of the drag coefficients from oscillating square cylinders (Ikeda *et al*, 1990), in order to decide upon a suitable drag coefficient. It is expressed by the following (Ikeda *et al*, 1990):

$$C_D\left(=C_p^+-C_p^-\right)=C_{D0}exp\left(-0.38\frac{b_{SK}}{l_{SK}}\right)$$

$$C_{D0}=\begin{cases}2.425Ke & (0\le Ke\le 2)\\ -0.3Ke+5.45 & (2<Ke)\end{cases}$$

$$C_p^+=1.2 \tag{70}$$

4.2.3 Multi-hull

Katayama *et al*. (2008) experimentally investigated the characteristics of roll damping of two types of multi-hull vessels: a high-speed catamaran; and a trimaran. They proposed a method of estimating the roll damping for these types of craft.

Wave making component

The wave making component B_{44W} is generated by the almost vertical motion of the demihull. For this component, the wave interaction between the hulls is considered significant, as also indicated by Ohkusu, (1970). However, for simplicity, this component can be estimated by using the heave potential damping of the demihull B_{33}. It should be noted however, that the B_{33} term does not include the wave interaction effects between the hulls. A strip method, including the end term effects, is used for the calculation of B_{33} (Katayama *et al*. 2008):

$$\begin{aligned}B'_{44\mathrm{W}}\dot{\varphi}&=B'_{44\mathrm{W}}\omega_\mathrm{E}\varphi_\mathrm{a}\\&=2b_\mathrm{demi}\ B'_{33}\ b_\mathrm{demi}\omega_\mathrm{E}\varphi_\mathrm{a}\\&=2{b_\mathrm{demi}}^2\ B'_{33}\dot{\varphi}\end{aligned} \tag{71}$$

where b_{demi} is the distance of the center of demihull from the vessel's center line.

Lift component

A method for the estimation of the lift component of a multi-hull vessel can be constructed based on Eq.(33). Based on the relative location of each hull in the multi-hull craft, l_R, l_0 and $\overline{O'G}$ are defined as shown in Fig. 9.

This allows the lift component to be described as follows (Katayama *et al*. 2008):

$$B_{44\mathrm{L}}=\frac{1}{2}\rho A_{\mathrm{HL}}Vk_\mathrm{N}l'_0\ l'_\mathrm{R}\left(1-1.4\frac{\overline{O'G}}{l'_\mathrm{R}}+0.7\frac{\overline{O'G}^2}{l'_0 l'_\mathrm{R}}\right) \tag{72}$$

$$k_N=\frac{2\pi d}{L_{PP}}$$

where $A_{\mathrm{HL}}$is the lateral area of the demi-hulls or side hulls under water line and L_{PP} isthe length between perpendiculars.

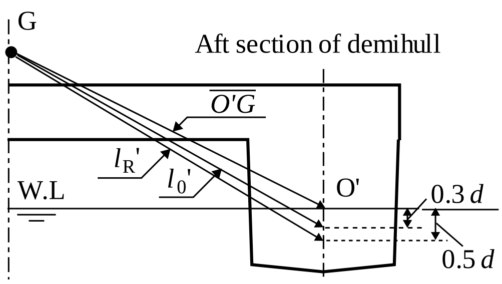

Fig. 9 Coordinate system to calculate l'$_0$ and l'$_\mathrm{R}$ and $\overline{O'G}$ (Katayama et al., 2008).

Frictional component

For multi-hull vessels, the frictional component is caused by the vertical motion of the demi-hull or side hull. This component is assumed to be smaller than the other components. Based on the estimation method proposed in the previous chapters, the friction component for the demi-hull or side hull can be estimated as follows (Katayama *et al*. 2008):

$$B'_{44\mathrm{F}} = \frac{8}{3\pi}\rho A_{\mathrm{HL}}\varphi_{\mathrm{a}}\omega_{\mathrm{E}} b_{\mathrm{demi}}{}^{3} C_{\mathrm{f}}\left(1 + 4.1\frac{V}{\omega_{\mathrm{E}} L_{\mathrm{PP}}}\right) \quad (73)$$

$$C_f = \frac{1.328}{\sqrt{Re}} \qquad Re = \frac{4\varphi_a b_{demi} d}{T_e \nu}$$

where A_{HL} is the lateral area of the demi-hulls or side hulls under water line, and $b_{\mathrm{demi}}$is the distance of the centre of the demi-hull from the centre line, ν is kinematic viscosity. The effects of forward speed can be taken into account with Eq.(41).

Eddy making component

Significant vortex shedding has been observed from flow visualization around multi-hull vessels whilst rolling. It was observed that one vortex was shed from each demi-hull of the catamaran and from each side hull of the trimaran. The location of the vortex shedding was found to be at the keel or the outside bilge of demi-hull/side hull. This is shown in Fig. 10 (Katayama *et al*. 2008).

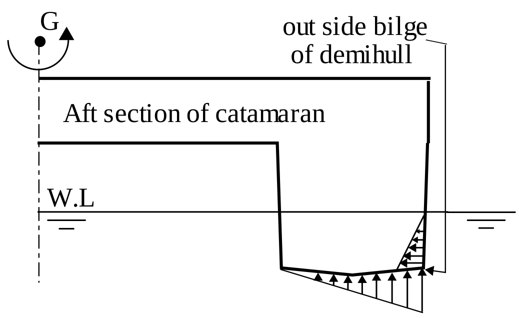

Fig. 10 Assumed vortex shedding point and pressure distribution of aft section of catamaran (Katayama et al., 2008).

The scale of the eddy may be similar to that for barge vessels. Therefore, these damping forces can be estimated by integrating the pressure caused by eddy-making phenomena over the hull surface. The pressure coefficient at the point of vortex shedding can be assumed to be 1.2 and the profile of pressure distribution is assumed as shown in Fig. 10. In addition, the effects of forward speed are taken into account by Eq. (45).

4.2.4 Additional damping for a planning hull

Typical planing craft have a shallow draught compared to their breadth, with an immersed lateral area that is usually very small. Even if the vessel runs at a very high speed, the horizontal lift component is small. Conversely, the water plane area is very large and the vertical lift force acting on the bottom of the craft is also large. As a result, this may play an important role in the roll damping. It is therefore necessary to take into account the component due to this effect. Assuming that a craft has small amplitude periodic roll motion about the centre of gravity, a point y on a cross section shown in Fig. 11, has a vertical velocity $u_z(y)$ [m/sec.] defined as:

$$u_z(y) = \dot{\varphi}\ y \quad (74)$$

where $\dot{\varphi}$ [rad./sec.] denotes roll angular velocity and y [m] is transverse distance between the centre of gravity and point y.

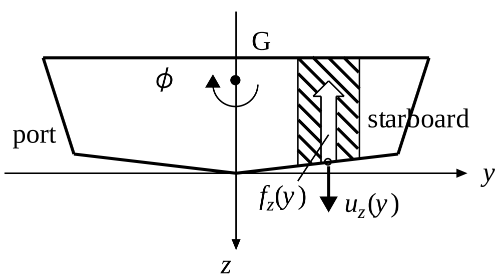

Fig. 11 Cross section of a ship (Ikeda et al., 2000).

When the craft has forward speed V [m/sec.], the buttock section including point y, experiences an angle of attack $\alpha(y)$ [rad] for the relative flow as shown in Fig. 12.

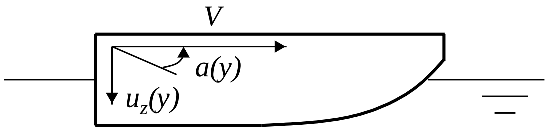

Fig. 12 Buttock section of a craft (Ikeda et al., 2000).

The angle $\alpha(y)$ can be calculated as follows:

$$\alpha(y) = \tan^{-1}\frac{u_z(y)}{V} = \tan^{-1}\frac{\dot{\varphi}y}{V} \cong \frac{\dot{\varphi}y}{V} \tag{75}$$

Assuming that the running trim angle is θ_1 [rad.], the vertical lift force acting on the craft is expressed as the virtual trim angle $\theta(y)$ [rad.] with the relative flow described as:

$$\theta(y) = \theta_1 + \alpha(y) \cong \theta_1 + \frac{\dot{\varphi}y}{V} \tag{76}$$

For planing craft, the magnitude of the hydrodynamic lift force significantly depends on the trim angle. The vertical lift force $f_z(y)$ [kgf/m] (positive upwards) acting on the buttock line including point y, with attack angle $\alpha(y)$ [rad.], is calculated as follows:

$$f_z(y) = \frac{1}{2}\rho B_{\mathrm{w.l}} V^2 k_{\mathrm{L}}(\theta_1)\alpha(y) \tag{77}$$

where ρ [kgf sec.^{2}/m^4] denotes the density of the fluid, $B_{\mathrm{w.l}}$ denotes the water line breadth and $k_{\mathrm{L}}(\theta_1)$ [1/rad.] is the lift slope. This is the non-dimensional vertical lift coefficient C_L differentiated by trim angle as follows:

$$k_{\mathrm{L}}(\theta_1) = \frac{\partial C_L}{\partial \theta} \tag{78}$$

On the basis of the quasi-steady assumption, $f_z(y)$[kgf/m] is assumed to be the mean value of the hydrodynamic lift force L [kgf] acting on the planning hull in steady running condition:

$$f_z(y) = \frac{L}{B_{\mathrm{w.l}}} = \frac{1}{2}\rho B_{\mathrm{w.l}} V^2 C_L \tag{79}$$

where the lever arm for the roll moment about the center of gravity is y [m]. The roll moment is then given by:

$$\begin{aligned} M_\phi &= \int_{-\frac{B_{\mathrm{w.l}}}{2}}^{\frac{B_{\mathrm{w.l}}}{2}} f_z(y) \cdot y\,dy \\ &= \frac{1}{24}\rho B_{\mathrm{w.l}}{}^4 V k_{\mathrm{L}}(\theta_1)\dot{\varphi} = B_{\mathrm{VL}}\dot{\varphi} \end{aligned} \tag{80}$$

This method of predicting the vertical lift component for planning craft is combined with the prediction method for a hard chine hull as an additional component $B_{44\mathrm{VL}}$ (Ikeda *et al*, 2000).

4.2.5 Additional damping for flooded ship

Flood water dynamics is similar to the effects of anti-rolling tank. The tank is classified according to its shape, such as a U-tube type or open-surface type. The ship motion including the effects of the tank has been theoretically established for each type (*e.g.* Watanabe, 1930, 1943; Tamiya, 1958; Lewison, 1976). However, in order to calculate the resultant ship motion, experiments such as forced oscillation tests are required to obtain some characteristics of the tank.

Based on experimental results by Katayama *et al*, (2009), and Ikeda *et al*, (2008) a proposed estimation formula for the roll damping component caused by flooded water was obtained. It should be noted that the prediction formula only applies to smaller roll angles but can be applied to cases without a mean heel angle.

$$B_{44\mathrm{IW}} = A(\frac{h}{B_{comp}}, \varphi_a, \frac{\overline{OG}}{B}) \times C(\omega_{\mathrm{E}}, \frac{h}{B_{comp}})^{B(\frac{h}{B_{comp}}, \varphi_a)} \times \exp\left\{-C(\omega_{\mathrm{E}}, \frac{h}{B_{comp}})^{B(\frac{h}{B_{comp}}, \varphi_a)}\right\} \times l_{\mathrm{comp}} \rho B_{\mathrm{comp}}^5 \sqrt{\frac{2g}{B_{\mathrm{comp}}}} \tag{81}$$

$$A(\frac{h}{B_{comp}}, \varphi_a, \frac{\overline{OG}}{B}) = \frac{1.8\frac{h}{B_{comp}} - 1.9882\varphi_a + 0.429}{1.2\frac{\overline{OG}}{B} + 1}$$

$$B(\frac{h}{B_{comp}}, \varphi_a) = 40.842\frac{h}{B_{comp}} - 10.502\varphi_a + 2.1$$

$$C(\omega_E, \frac{h}{B_{comp}}) = \frac{1}{\pi}\sqrt{\frac{B}{g}} \cdot \left(\frac{\omega_E}{\sqrt{h/B_{comp}}}\right) = \frac{\omega_E}{\omega_{IW}}$$

$$\omega_{IW} = \frac{\pi}{B_{comp}}\sqrt{gh}$$

where h is water depth. l_{comp} and B_{comp} are the length and the breadth of flooding compartment. ρ and g are the density of fluid and acceleration of gravity respectively. ω_{E} is roll frequency, ϕ_{a} is roll amplitude, ω_{IW} is the natural frequency of the water in a tank.

4.3 Simplified Ikeda's Method

This method is a simplification of the Ikeda's Method for displacement-type monohulls, described in Section 4.2.1, which was deducted by using regression analysis and using methodical series of ships (Kawahara et al., 2009). Validation of program of simplified Ikeda's method can be done using Taylor Standard Series data.

In this section, a roll damping coefficient with subscript 0 (e.g.$B_{44,\mathrm{E},0}$ $[(N \cdot m)/s]$) indicates a value at zero forward speed.

Formulas in Sections 4.3.1, 4.3.4 and 4.3.5 are applicable for the following range of hull particulars:

$$\begin{pmatrix} 0.50 \le C_B \le 0.85; & 0.90 \le C_M \le 0.99 \\ 2.5 \le B/d \le 4.5; & -1.5 \le \overline{OG}/d \le 0.2 \end{pmatrix} \tag{82}$$

where C_B $[nd]$ is the block coefficient, C_M $[nd]$ is the midship section coefficient, B/d $[nd]$ is the ratio breadth to draught, $\overline{OG}/d$ $[nd]$ is the ratio of the $\overline{OG}$ $[m]$ to draft, being $\overline{OG}$ defined by the difference between water surface and the center of gravity ($\overline{OG} = d - \overline{KG}$).

Moreover, formulas in Section 4.3.5 are only applicable for the following range of bilge keel main dimensions:

$$\begin{pmatrix} 0.01 \le b_{BK}/B \le 0.06 \\ 0.05 \le l_{BK}/L \le 0.40 \end{pmatrix} \tag{83}$$

where b_{BK} $[m]$ is the width of the bilge keel and l_{BK} $[m]$ is the length of the bilge keel.

4.3.1 Wave component

The wave component at zero forward speed is given by the following equation:

$$\hat{B}_{44,W,0} = \frac{A_1}{\hat{\omega}_E} \cdot \exp(-0.6944 \cdot A_2 \cdot (\log(\hat{\omega}_E) - A_3)^2) \tag{84}$$

where:

$$x_1 = B/d \qquad x_2 = C_B \qquad x_3 = C_M \qquad x_4 = 1 - \overline{OG}/d \tag{85}$$

$$A_1 = AA_1 \cdot \sum_{i=1}^{3}\sum_{j=1}^{4}\sum_{k=1}^{5} Q1_{j+4\cdot(i-1),k} \cdot x_1^{5-k} \cdot x_2^{4-j} \cdot x_4^{3-i} \tag{86}$$

$$AA_1 = 1.0 + (1 - x_4) \cdot \sum_{i=1}^{2}\sum_{j=1}^{3}\sum_{k=1}^{5} Q1_{j+3\cdot i+9,k} \cdot x_1^{5-k} \cdot x_2^{3-j} \cdot x_3^{2-i} \tag{87}$$

$$A_2 = \sum_{i=1}^{5} Q2_i \cdot x_4^{5-i} \tag{88}$$

$$A_3 = AA_3 + \sum_{i=1}^{7}\sum_{j=1}^{7} Q3_{i,j} \cdot x_2^{7-j} \cdot x_4^{7-i} \tag{89}$$

$$AA_3 = \sum_{i=1}^{4} Q4_{1,i} \cdot x_1^{4-i} \cdot \sum_{j=1}^{2}\sum_{k=1}^{4} Q4_{4-j,k} \cdot x_2^{4-k} \cdot x_4^{j-1} \cdot \left(\sum_{i=1}^{10} Q5_i \cdot \left(x_4 - \sum_{j=1}^{4} Q4_{4,j} \cdot x_1^{4-j}\right)^{10-i} + \sum_{i=1}^{3} Q5_{i+9} \cdot x_1^{3-i} \right) \tag{90}$$

Factors Q1 and Q2 are available in Table 1. The first index of the factor Q1refers to the line number in Table 1while the second index of the factor Q1 (k) refers to the column number in Table 1.

Factors Q3 are placed in Table 2. The first index of the factor Q3 (i), refers to the line number in Table 2, while the second index of the factor Q3 (j), refers to the column number in Table 2. Factors Q4 and Q5 are available from Table 3. The first index of the factor Q4 refers to the line number in Table 3, while the second index of the factor Q4 refers to the column number in Table 3. The index for the factor Q5 is located above the values in Table 3.

4.3.2 Lift component

The lift component is given by the following formulation:

$$B_{44,\mathrm{L}} = \frac{\rho}{2} \cdot V \cdot L \cdot d \cdot k_{\mathrm{N}} \cdot l_0 \cdot l_{\mathrm{R}} \cdot \left[1.0 - 1.4 \cdot \frac{\overline{OG}}{l_{\mathrm{R}}} + \frac{0.7 \cdot \overline{OG}^2}{l_0 \cdot l_{\mathrm{R}}}\right] \tag{91}$$

where ρ $[kg/m^3]$ is the density of the fluid and V $[m/s]$ is the ship's velocity and where:

$$l_0 = 0.3 \cdot d \quad ; \quad l_{\mathrm{R}} = 0.5 \cdot d \tag{92}$$

$$k_{\mathrm{N}} = 2 \cdot \pi \cdot \frac{d}{L} + \kappa \cdot \left(4.1 \cdot \frac{B}{L} - 0.045\right) \tag{93}$$

$$\kappa = \begin{cases} 0.0 & C_M \leq 0.92 \\ 0.1 \quad for & 0.92 < C_M \leq 0.97 \\ 0.3 & 0.97 < C_M \end{cases} \tag{94}$$

4.3.3 Frictional component

The frictional component at zero forward speed is given by the following formulation:

$$B_{44,\mathrm{F},0} = \frac{4}{3 \cdot \pi} \cdot \rho \cdot s_{\mathrm{f}} \cdot r_{\mathrm{f}}^3 \cdot \varphi_{\mathrm{a}} \cdot \omega_{\mathrm{E}} \cdot c_{\mathrm{f}} \tag{95}$$

where:

$$c_{\mathrm{f}} = 1.328 \cdot \left(\frac{3.22 \cdot r_{\mathrm{f}}^2 \cdot \varphi_{\mathrm{a}}^2}{T_E \cdot \nu}\right)^{-0.5} \tag{96}$$

$$r_{\mathrm{f}} = \frac{1}{\pi} \cdot \left((0.887 + 0.145 \cdot C_M) \cdot (1.7 \cdot d + C_M \cdot B) - 2 \cdot \overline{OG} \right) \tag{97}$$

$$s_{\mathrm{f}} = L \cdot (1.75 \cdot d + C_M \cdot B) \tag{98}$$

where T_E $[s]$ is the roll circular period and ν $[m^2/s]$ is the kinematic viscosity of water.

In Kawahara et al. (2009), there is an erratum in Eq. (21) of the paper, the corrected Equation is in this document, Eq. (96).

4.3.4 Eddy making component

The eddy component at zero forward speed is given by the following equation:

$$\hat{B}_{44,E,0} = \frac{4 \cdot \hat{\omega}_E \cdot \varphi_a}{3 \cdot \pi \cdot x_2 \cdot {x_1}^3} \cdot C_R \tag{99}$$

where:

$$x_1 = B/d \quad x_2 = C_M \quad x_3 = C_M \quad x_4 = \frac{\overline{OG}}{d} \tag{100}$$

$$C_R = A_E \cdot \exp(B_{E1} + B_{E2} \cdot {x_3}^{B_{E3}}) \tag{101}$$

$$A_E = (-0.0182 \cdot x_2 + 0.0155) \cdot (x_1 - 1.8)^3 + \sum_{i=1}^{5} Q6_{1,i} \cdot x_2^{5-i} \tag{102}$$

$$B_{E1} = (-0.2 \cdot x_1 + 1.6) \cdot (3.98 \cdot x_2 - 5.1525) \cdot x_4 \cdot \left(x_4 \cdot \sum_{i=1}^{3} Q6_{2,i} \cdot x_2^{3-i} + \sum_{i=1}^{2} Q6_{2,i+3} \cdot x_2^{2-i} \right) \tag{103}$$

$$B_{E2} = (0.25 \cdot x_4 + 0.95) \cdot x_4 + \sum_{i=1}^{5} Q6_{3,i} \cdot x_2^{5-i} \tag{104}$$

$$B_{E3} = (46.5 - 15 \cdot x_1) \cdot x_2 + 11.2 \cdot x_1 - 28.6 \tag{105}$$

Factors Q6 are placed in Table 4. The first index of the factor Q6 refers to the line number in Table 4, while the second index of the factor Q6 refers to the column number Table 4.

4.3.5 Bilge keel component

The bilge keel component at zero forward speed is given by the following equation:

$$\hat{B}_{44,BK,0} = A_{BK} \cdot \hat{\omega}_E \cdot \exp(B_{BK1} + B_{BK2} \cdot {x_3}^{B_{BK3}}) \tag{106}$$

where:

$$x_1 = B/d \;;\quad x_2 = C_B \;;\quad x_3 = C_M; \quad x_4 = \frac{\overline{OG}}{d} \;;\quad x_6 = \varphi_a \text{ [deg]}; \quad x_7 = b_{BK}/B \;;\quad x_8 = l_{BK}/L \tag{107}$$

$$A_{BK} = f_1 \cdot f_2 \cdot f_3 \tag{108}$$

$$f_1 = (x_1 - 2.83)^2 \cdot \sum_{i=1}^{3} Q7_{1,i} \cdot x_2^{3-i} + \sum_{i=1}^{3} Q7_{2,i} \cdot x_2^{3-i} \tag{109}$$

$$f_2 = \sum_{i=1}^{3} Q7_{3,i} \cdot x_6^{3-i} \tag{110}$$

$$B_{BK1} = x_4 \cdot \left(5 \cdot x_7 + 0.3 \cdot x_1 - 0.2 \cdot x_8 + \sum_{i=1}^{3} Q7_{6,i} \cdot x_6^{3-i} \right) \tag{111}$$

$$B_{BK2} = -15 \cdot x_7 + 1.2 \cdot x_2 - 0.1 \cdot x_1 + \sum_{i=1}^{3} Q7_{7,i} \cdot {x_4}^{3-i} \tag{112}$$

$$B_{BK3} = 2.5 \cdot x_4 + 15.75 \tag{113}$$

Factors Q6 are placed in Table 5. The first index of the factor Q7 refers to the line number in Table 5while the second index of the factor Q7 refers to the column number in Table 5.

5. VALIDATION

5.1 Uncertainty Analysis

Uncertainty analysis should be performed in accordance with the ‘Guide to the Expression of Uncertainty Analysis in Experimental Hydrodynamics’ 7.5-02-01-01.

5.2 Benchmark Model Test Data

Some benchmark data is available for the empirical methods to estimate roll damping. In the following, the model tests data is summarized:

- Wave making component and lift component: Ikeda *et al.*, (1978a).
- Frictional component: no benchmark model test data is available.
- Eddy making component: Ikeda et al., (1977a) or (1978b).
- Appendages component: regarding bilge keel component, refer to Ikeda et al., (1976, 1977b or 1978d); and regarding skeg component, refer to Ali et al., (2004).
- Hard chine hull: Ikeda et al.,(1990) or Tanaka et al., (1985).
- Multi-hull: Katayama et al, (2008).
- Planning hull: Ikeda et al., (2000).
- Frigate: Etebari et al., (2008), Bassler et al., (2007), Grant et al., (2007), Atsavapranee et al., (2007) or (2008).
- Water on deck or water in tank: Katayama et al, (2009).

For full-scale data, refer to Atsavapranee *et al*., (2008), where flow visualization around bilge keel and free decay test results are indicated.

6. DOCUMENTATION

The results from the tests or estimations should be collated in a report, which should contain at least the following information:

- Model specifications:
  - Identification
  - Loading condition: weight or draught, height of the centre of gravity $\overline{KG}$, (undamped) roll natural period T_φ or frequency ω_x
  - Model scale
  - Main dimensions and hydrostatics of the model, including the characteristics of the appendages used (see recommendations of ITTC Standard Procedure 7.5-01-01-01, Ship Models)
- Test date (if tests have been performed)
- Particulars of the towing tank, including length, breadth and water depth (if tests have been performed)
- Parametric data for the tests/estimations:
  - Water temperature of tank water
  - Density of tank water
  - Kinematic viscosity of the water
- For each test/estimation:
  - Rolling conditions: excitation period T_E or frequency ω_E, wave direction χ, forward speed V or Froude number F_r and roll amplitude φ_a

7. LIST OF SYMBOLS

A_{M}	midship section area
A_{HL}	lateral area of the demihulls or side hulls under water line
A_{j}	area of cross section under water line
a	length acting on C_{fp} sectional girth length from keel to hard chine or water line
a_1, a_3	Lewis-form parameter
B	breadth of the ship
B_{33}	linear coefficient of heave damping
B_{44}	equivalent linear damping component
$\hat{B}_{44}$	non-dimensional equivalent linear damping component
$B_{44\mathrm{BKL}}$	equivalent linear coefficient of bilge-keel lift component of roll damping
$B_{44\mathrm{BKW}}$	equivalent linear coefficient of bilge-keel wave making component of roll damping
$B_{44\mathrm{VL}}$	equivalent linear coefficient of vertical lift component of roll damping
$B_{44,\mathrm{W}}$	equivalent linear wave roll damping
$B_{44,\mathrm{L}}$	equivalent linear wave roll damping
$B_{44,\mathrm{F}}$	equivalent linear friction roll damping
$B_{44,\mathrm{E}}$	equivalent linear eddy roll damping
$B_{44,\mathrm{App}}$	equivalent linear appendages roll damping
$B_{44,\mathrm{BK}}$	equivalent linear bilge keel roll damping
$B_{44,\mathrm{E},0}$	equivalent linear eddy roll damping at zero forward speed

B'_{22} [prime ’] indicates sectional value sectional equivalent linear coefficient of sway damping

B'_{33} sectional linear coefficient of heave damping

B'_{42} sectional equivalent linear coupling coefficient of roll damping by swaying

B'_{44} sectional linear coefficient of total roll damping

$B'_{44\mathrm{F}}$ sectional equivalent linear coefficient of frictional component of roll damping

$B'_{44\mathrm{W}}$ sectional equivalent linear coefficient of wave making component of roll damping

$B'_{44\mathrm{BKH0}}$ sectional equivalent linear coefficient of bilge-keel’s hull pressure component of roll damping without forward speed

$B'_{44\mathrm{BKN0}}$ sectional equivalent linear coefficient of bilge-keel’s normal force component of roll damping without forward speed

$B'_{44\mathrm{E0}}$ sectional equivalent linear coefficient of eddy making component of roll damping without forward speed

$B'_{44\mathrm{F0}}$ sectional equivalent linear coefficient of frictional component of roll damping without forward speed

$B'_{44\mathrm{SK0}}$ sectional equivalent linear coefficient of skeg component of roll damping without forward speed

$B'_{44\mathrm{W0}}$ sectional equivalent linear coefficient of wave making component of roll damping without forward speed

b_{BK} width of the bilge keel

B_{comp} breadth of flooding component

B_{eq} equivalent linear damping component

$B_{\mathrm{w.l}}$ water line breadth

b_{SK} thickness of skeg

b_{demi} distance from the centre line to the centre of demihull

$B(\dot{\varphi})$ damping moment function, assumed to be de-pendent only on the instantaneous roll velocity

$B_{\varphi,n}$ nonlinear damping components

$B_{\varphi,W}$ wave component of roll damping

$B_{\varphi,L}$ lift component of roll damping

$B_{\varphi,F}$ friction component of roll damping

$B_{\varphi,E}$ eddy component of roll damping

$B_{\varphi,App}$ appendages component of roll damping

$B_{\varphi,BK}$ bilge keel component of roll damping

C_{44} restoring moment

c_{44} normalized restoring moment

C_{B} block coefficient

$C_{\mathrm{BK}}(b_{\mathrm{BK}})$ source strength C_{BK}(a function of b_{BK})

C_D drag coefficient of something

C_{D0} drag coefficient of skeg or flat plate without thickness

C_{f} frictional resistance coefficient

c_g group speed

C_L vertical lift coefficient

C_M midship section coefficient

C_p pressure coefficient

C_p^- negative pressure coefficient behind of bilge keel

C_p^- pressure coefficient behind skeg

C_p^+ positive pressure coefficient front of bilge keel

C_p^+ pressure coefficient front of the skeg

C_{R} drag coefficient proportional to velocity on surface of rotating cylinder

d draught of the ship

$d_{\mathrm{BK}}(\phi)$ depth of the position attached bilge-keel on hull

d_{c} depth of chine

$d(\dot{\varphi})$ normalized damping moment function dependent on the instantaneous roll velocity

f correction factor to take account of the increment of flow velocity at bilge

$f_1(\alpha)$ modification coefficient as a function of the rise of floor (S)

$f_2(\alpha)$ modification coefficient as a function of the rise of floor (C_{p})

f_E frequency of motion or of the incident wave

$f_{\mathrm{z}}(y)$ vertical lift force acting on the buttock line including point $A(y)$,with attack angle $\alpha(y)$ [rad.]

g acceleration of gravity

G the center of gravity
G girth length
GM metacentric height with respect to the ship centre of gravity
GZ hydrostatic roll righting lever with respect to the centre of gravity of the ship
H_0 half breath draught ratio $H_0 = B / (2d)$
$(I_{44} + \partial I_{44})$ total roll moment of inertia, including the hydrodynamic added inertia along a longitudinal axis through the centre of gravity
h Water depth
K reduced frequency $K = \omega L / U$
K_a external transversal moment amplitude in forced roll tests
K_e Keulegan-Carpenter number
k_L, $k_L(\theta_1)$ lift slope of vertical lift (for planing hull)
k_N lift slope of horizontal lift (ship in maneuvering)
L hydrodynamic lift force acting on planing hull
L_{BK} lift force acting on a bilge keel
l distance from the centre of gravity or roll to the tip of skeg or the tip of bilge-keel or chine
l_0 lever defined that the quantity $l_0\dot{\varphi}/U$ corresponds to the angle of attack of the lifting body
l_0' distance from the center of gravity to the point of 0.5d on center line of demihull
l_1 distance from the centre of gravity or roll to the centre of skeg or bilge-keel
l_2 moment lever integrated pressure along hull surface front of skeg or baseline
l_3 moment lever integrated pressure along hull surface behind skeg or baseline
l_{comp} length of flooding component
l_p moment lever betweenn the centre of gravity or roll and the centre of integrated pressure along hull
l_{BK} distance from the centre of gravity or roll to the position attached bilge-keel on hull
l_R distance from still water level to the centre of lift
l_R' distance between the center of gravity and the cross point of 0.7d water line and the center line of a demihull
l_{SK} height of skeg
l_w moment lever measured from the still water level due to the sway damping force
$M_{\varphi APP}$ appendage component of roll damping
$M_{\varphi E}$ eddy making component of roll damping
$M_{\varphi F}$ frictional component of roll damping
$M_{\varphi L}$ lift component of roll damping
$M_{\varphi W}$ wave making component of roll damping
$N(\varphi_a)$ Bertin's roll damping coefficient
O origin of the fixed coordinate system on ship (the point on still water level)
O' origin of the fixed coordinate system on demihull (the point on still water level)
$\overline{O'G}$ distance from O' to G
P_m pressure on hull caused by vortex shedding
R bilge radius
Re Reynolds number
RMG roll moment generator
r radius of cylinder
$r(\varphi)$ ratio between the hydrostatic roll righting lever and the metacentric height
S length of pressure distribution on cross section
S_0 length of negative-pressure region
T_φ (undamped) ship roll natural period
T_E roll circular period of a steady periodic oscillation (steady roll frequency)
U_{max} amplitude of motion velocity or maximum speed of something
u maximum speed of the tip of bilge-keel
$u_z(y)$ vertical velocity at a point $A(y)$
V ship speed
V_R relative flow velocity $V_R^2 = U^2 + u^2$
V_{max} maximum relative velocity on the hull surface
V_{mean} mean velocity on the hull surface
y transverse distance between the centre of gravity and point $A(y)$
y lever arm for the roll moment
α Attack angle $\alpha = \tan^{-1}(u/U)$

β rise of floor (deadrise angle)
$\alpha(y)$ experiences an angle of attack
δ discrepancy
γ ratio of maximum velocity to mean velocity on hull surface $\gamma = V_{\max} / V_{\text{mean}}$
γ_n nonlinear restoring coefficients
κ modification factor of midship section coefficient
$\theta(y)$ virtual trim angle
θ_1 running trim angle
σ area coefficient $\sigma = A_j / (Bd)$
φ roll angle
φ_a roll amplitude of a steady periodic oscillation (steady roll amplitude)
φ_{res} resonance peak amplitude
ψ Lewis argument on the transformed unit circle
φ equivalent linear damping coefficient
φ_a kinematic viscosity of water
ω_{IW} natural circular frequency of water in a tank $\omega_{\text{IW}} = \frac{\pi}{B_{comp}}\sqrt{gh}$
ω_E roll circular frequency of a steady periodic oscillation (steady roll frequency)
$\widehat{\omega}_E$ non-dimensional roll circular frequency of a steady periodic oscillation (steady roll frequency)
ω_{res} resonance peak frequency
ω_x (undamped) ship roll natural frequency
$\omega_{x,eq}$ equivalent undamped ship's roll natural frequency
ρ mass density of water
$\sigma_{\dot{x}}$ standard deviation of the roll velocity
Δ ship displacement
ΔT_{ref} estimated time windowing of forced roll tests
∇ ship displacement volume

8. REFERENCES

Ali, B., Katayama, T., Ikeda, Y., 2004, "Roll damping characteristics of fishing boats with and without drift motion", International Shipbuilding Progress, Vol. 51 (2/3), pp.237-250.

Atsavapranee, P., Carneal, J.B., Grant, D.J., Percival, S., 2007, "Experimental Investigation of Viscous Roll Damping on the DTMB Model 5617 Hull Form", Proceedings of the 26th International Conference on Offshore Mechanics and Arctic Engineering, OMAE2007-29324

Atsavapranee, P., Grant, D.J., Carneal, J.B., Etebari, A., Percival, S., Beirne, T., 2008, "Full Scale Investigation of Bilge Keel Effectiveness at Forward Speed", NSWCCD-50-TR-2008 / 075.

Bassler, C.C., Carneal, J.B., Atsavapranee, P., 2007, "Experimental Investigation of Hydrodynamic Coefficient of a Wave-piercing Tumble Hull Form", ASME 26th International Conference on Offshore Mechanics and Arctic Engineering, Vol. 4, Paper No. OMAE2007-29310, pp. 537-548.

Bassler, C.C, Reed, A.M., 2009, "An Analysis of the Bilge Keel Roll Damping Component Model", Proceedings of 10th International Conference on Stability of Ships and Ocean Vehicles, pp.369-385, St. Petersburg.

Bassler, C.C., Reed, A.M., 2010, "A Method to Model Large Amplitude Ship Roll Damping", Proceedings of the 11th International Ship Stability Workshop, pp.217-224.

Bertgalia, G., Scarpa, G., Serra, A., Francescutto, A., Bulian, G., 2004, "Systematic Experimental Tests for IMO Weather Criterion Requirements and Further Development Towards a Probabilistic Intact Stability Approach", Proceedings of the 7th International Ship Stability Workshop, Shanghai, China, pp. 63-74.

Bertin L.E., 1874a, "Naval Science", Vol. III, pp.198.

Bertin L.E., 1874b, "Donnees théoriques Et Expérimentales Sur Les Vagues Et Le Roulis", Kessinger Legacy Reprints.

Blasius, H., 1908, "The Boundary Layers in Fluids with Little Friction", Zeitschrift fuer Mathematik und Physik, Band 56, Vol. 1, pp.1-37 (in German).

Blasius, H., 1950, "The Boundary Layers in Fluids with Little Friction", National Advisory Committee For Aeronautics, Technical Memorandum 1256, pp.1-58.

Blume, P., 1979, "Determination of Coefficients for the Effective Roll Damping by Model Tests and their Application for Estimating Large Roll Angles", Schiffstechnik Bd. 26, pp. 3-23 (in German)

Bulian, G., 2004, "Estimation of Nonlinear Roll Decay Parameters Using an Analytical Approximate Solution of the Decay Time History", International Shipbuilding Progress, 51(1), pp. 5-32.

Bulian, G., Francescutto, A., Fucile, F., 2009, "Project HYD-III-CEH-5: Determination of Relevant Parameters for the Alternative Assessment of Intact Stability Weather Criterion on Experimental Basis",Project Report, HYDROLAB Project.

Etebari, A., Atsavapranee, P., Bassler, C.C., Carneal, J., 2008, "Experimental Analysis of Rudder Contribution to Roll Damping", Proceedings of the ASME 27th International Conference on Offshore Mechanics and Arctic Engineering, No. OMAE2008-57265, pp. 165-174.

Froude, W., Abell, W., Gawn, R., Duckworth, A., 1955, "The Papers of William Froude, 1810-1879: With a Memoir by Sir Westcott Abell and an Evaluation of William Froude's Work by R.W.L. Gawn - On Resistance in Rolling of Ships", Institution of Naval Architecture.

Gawn, R. W. L., 1940, "Rolling Experiments with Ships and Models in Still Water", Trans. I.N.A., 82.

Grant, D.J, Etebari, A.,Atsavapranee, P., 2007, "Experimental Investigation of Roll and Heave Excitation Damping in Beam Wave Fields", Proceedings of the 26th International Conference on Offshore Mechanics and Arctic Engineering, No. OMAE2007-29318, pp. 549-559.

Grant, D., Bassler, C.C., Percival, S., Walker, D., 2010, "Design and Use of a 3DoF Motion Mechanism for Large Amplitude Forced Oscillation Model Testing", Proceedings of the 29th American Towing Tank Conference, pp. 199-206.

Handschel, S., Abdel-Maksoud, M., 2014a, "Improvement of the harmonic excited roll motion technique for estimating roll damping", Ship Technology Research, Vol. 61 (3), pp. 116-130.

Handschel, S., Abdel-Maksoud, M., Fröhlich, M., 2014b, "Experimental and Numerical Investigation of Ship Roll Damping by Applying the Harmonic Forced Roll Motion Technique", Proceedings of the 30th Symposium on Naval Hydrodynamics (SNH2014), Hobart, Tasmania, Australia.

Haddara, M.R., 2005, "Roll damping: a review", Oceanic Engineering International, 9(1), pp. 1-10.

Hashimoto, H., Sanya Y., 2009, "Research on Quantitative Prediction of Parametric Roll in Regular Waves", Conference Proceedings of the Japan Society of Naval Architects and Ocean Engineers, Vol.8, pp.361-364.

Himeno, Y., 1981, "Prediction of Ship Roll Damping- State of the Art", Technical Report 239, College of Engineering, The University of Michigan, Michigan, USA.

Hughes, G., 1954, "Friction and Form Resistance in Turbulent Flow, and a Proposed Formulation for use in model and Ship Correlation", National Physical Laboratory, NPL, Ship Division, Paper No. 7, London, April, RINA Transactions 1954-16.

Idle, G., Baker, G.S., 1912, TINA, 54, pp.103.

Ikeda, Y., Himeno, Y., Tanaka, N., 1976, "On Roll Damping Force of Ship: Effects of Friction of Hull and Normal Force of Bilge Keels", Journal of the Kansai Society of Naval Architects, Vol.161, pp.41-49 (in Japanese).

Ikeda, Y., Himeno, Y., Tanaka, N., 1977a, "On Eddy Making Component of Roll Damping Force on Naked Hull", Journal of the Society of Naval Architects of Japan, Vol.142, pp.54-64 (in Japanese).

Ikeda, Y., Komatsu, K., Himeno, Y., Tanaka, N., 1977b, "On Roll Damping Force of Ship -Effects of Hull Surface Pressure Created by Bilge Keels", Journal of the Kansai Society of Naval Architects, Vol. 165, pp.31-40 (in Japanese).

Ikeda, Y., Himeno, Y., Tanaka, N., 1978a, "Components of Roll Damping of Ship at Forward Speed", Journal of the Society of Naval Architects of Japan, Vol.143, pp.113-125 (in Japanese)

Ikeda Y., Himeno Y., Tanaka N., 1978b, "On Eddy Making Component of Roll Damping Force on Naked Hull", Journal of the Society of Naval Architects of Japan, Vol. 142, pp. 54-64 (in Japanese).

Ikeda, Y., Himeno, Y., Tanaka, N., 1978c, "A Prediction Method for Ship Roll Damping", Report No. 00405, Department of Naval Architec-ture University of Osaka Prefecture, pp. 1-23.

Ikeda, Y., Himeno, Y., Tanaka, N., 1978d, "On Roll Damping Force of Ship -Effects of Hull Surface Pressure Created by Bilge Keels", Report of Department of Naval Architecture University of Osaka Prefecture, No. 00402.

Ikeda, Y., Umeda, N., 1990, "A Prediction Method of Roll Damping of a Hard-chine Boat at Zero Forward Speed", Journal of the Kansai Society of Naval Architects, Vol.213, pp.57-62 (in Japanese).

Ikeda Y., Fujiwara T., Katayama T., 1993, "Roll damping of a sharp cornered barge and roll control by a new-type stabilizer", Proceedings of the 3rd International Society of Offshore and Polar Engineers Conference, Vol. 3, pp. 634-639, Singapore.

Ikeda, Y., Katayama, T., Hasegawa, Y., Segawa, M., 1994, "Roll Damping of High Speed Slender Vessels", Journal of the Kansai Society of Naval Architects, Vol. 222, pp.73-81 (in Japanese).

Ikeda, Y., Katayama, T., 2000, "Roll Damping Prediction Method for a High-Speed Planning Craft", Proceedings of the 7th International Conference on Stability of Ship and Ocean Vehicles, B, pp.532-541.

Ikeda, Y., Kawahara, Y., 2008, "A Proposal of Guidance to the Master of a Damaged Passenger Ship for Deciding to Return to Port", Journal of the Japan Society of Naval Architects and Ocean Engineers, Vol.7, pp.115-122 (in Japanese).

IMO SLF 47/6/8. Review of the Intact Stability Code: Guidelines for model testing of Intact Stability. Experimental approach to evaluate the relevant factors for the calculation of the roll angle θ_1 ", Submitted by Italy, June 2004, London

IMO MSC.1/Circ. 1200. Interim Guidelines for Alternative Assessment of the Weather Criterion, May 2006, London

JSRA (Japan Shipbuilding Research Association), 1977, Reports of Committee SR 161. no 27 (in Japanese).

Kaplan, P., 1966, Nonlinear Theory of Ship Roll Motion in a Random Seaway, Webb Institute, Lecture Notes.

Katayama, T., Taniguchi, T., 2008, "A Study on Viscous Effects of Roll Damping for Multi-Hull High-Speed Craft", Journal of the Japan Society of Naval Architects and Ocean Engineers, Vol.8, pp.147-154 (in Japanese).

Katayama, T., Kotaki, M., Katsui, T., Matsuda A., 2009, "A Study on Roll Motion Estimation of Fishing Vessels with Water on Deck", Journal of the Japan Society of Naval Architects and Ocean Engineers, Vol. 9, pp. 115-125 (in Japanese).

Katayama, T., Yoshida, N., Yamamoto, Y., Kashiwagi, M., Ikeda, Y., 2022, "Correction of Eddy Making Component of Ikeda's method and its Modification for Shallow Draught Effects", Proceedings of the 18th International Ship Stability Workshop, Gdansk, Poland.

Kato, H., 1957, "On the Frictional Resistance to the Rolling of Ships", Journal of Zosen Kyokai, Vol.102, pp.115-122 (in Japanese).

Kawahara, Y., Maekawa, K., Ikeda, Y., 2009, "A Simple Prediction Formula of Roll Damping of Conventional Cargo Ships on the Basis of Ikeda's Method and Its Limitations", Proceedings of the 10th International Conference on Stability of Ships and Ocean Vehicles, pp. 387-398.

France, W. M, M. Levadou, T. W. Treakle, J. R. Paulling, K. Michel and C. Moore (2003). An Investigation of Head-Sea Parametric Rolling and its Influence on Container Lashing Systems. Marine Technology, Vol. 40, No 1, pp. 1–19.

Lewison, G.R.G., 1976, "Optimum Design of Passive Roll Stabilizer Tanks", Naval Architect, Vol. 1, pp. 31-45.

Luthy, V., Grinnaert, F., Billard, J. Y., Delhaye, T., Claudel, R. and J. F. Leguen, 2021, "An iterative method to estimate damping coefficients from roll decay time series", Proceedings of the 1st International Conference on the Stability and Safety of Ships and Ocean Vehicles (STABS 2021), Glasgow, UK.

Ohkusu, M., 1970, "On the Motion of Multihull Ship in Wave", Transactions of the West-Japan Society of Naval Architects, Vol.40, pp.19-47 (in Japanese).

Oliva-Remola, A., Bulian, G., Pérez-Rojas, L., 2018, "Estimation of damping through internally excited roll tests", Ocean Engineering, 160, pp. 490-506.

Oliveira, M., Kassar, B., Coelho, L., Monteiro, F., Santis, R., Rodriguez, C., Neves, M., Polo, J. and P. Esperança, 2018, "Empirical and experimental roll damping estimates for an oil tanker in the context of the 2nd generation intact stability criteria", Proceedings of the 13th International Conference on Stability of Ships and Ocean Vehicles (STAB2018), September 16-21, Kobe, Japan, pp. 179-191.

Roberts, J., 1985, "Estimation of Nonlinear Ship Roll Damping from Free-Decay Data", Journal of Ship Research, Vol. 29, No 2, pp. 127-138.

Standing, R.G., 1991, "Prediction of viscous roll damping and response of transportation barges in waves", Proceedings of the 1st International Society of Offshore and Polar Engineers Conference, Vol. 3, August, Edinburgh.

Söder, C.-J., Rosén, A., Werner, S., Huss, M., Kuttenkeuler, J., 2012, "Assessment of Ship Roll Damping through Full-Scale and Model-Scale Experiments and Semi-Empirical Methods", Proceedings of the 11th International Conference on Stability of Ships and Ocean Vehicles, Athens, Greece, pp. 877-886.

Takaki M., Tasai F., 1973, "On the Hydrodynamic Derivative Coefficients of the Equations for Lateral Motions of Ships", Transactions of the West Japan Society of Naval Architects, Vol. 46 (in Japanese).

Tamiya, S., 1958, "On the Dynamical Effect of Free Water Surface", Journal of Zosen Kyokai, Vol. 103, pp. 59-67 (in Japanese).

Tamiya, S., Komura, T., 1972, "Topics on Ship RollingCharacteristics with Advance Speed", Journal of the Society of Naval Architects of Japan, Vol.132, pp.159-168 (in Japanese).

Tanaka, N., Ikeda, Y., 1985, "Study on Roll Characteristics of Small Fishing Vessel: Part 4 Effect of Skeg and Hard-chine on Roll Damping", Journal of the Kansai Society of Naval Architects, Vol. 196, pp. 31-37 (in Japanese).

Tasai, F., 1965, "Equation of Ship Roll Motion", Research Institute for Applied Mechanics, Kyushu University, Report No. 25 (in Japanese).

Motora, S., 1964, Theory of Ship Motion, Kyoritsu Shuppan Book Co. (in Japanese).

Wu, X., Tao, L., Li, Y., 2005, "Nonlinear Roll Damping of Ship Motions in Waves", Journal of Offshore Mechanics and Arctic Engineering, Vol. 127, No 3, pp. 205-211.

Yamashita, S., Katagiri, T., 1980, "The results of a systematic series of tests on rolling motion of a box-shaped floating structure of shallow draught", Transactions of West Japan Society of Naval Architects, Vol. 60, pp. 77-86.

Vassilopoulos, L., 1971 "Ship Rolling at Zero Speed in Random Beam Seas with Nonlinear Damping and Restoration", Journal of Ship Research, Vol. 15 No. 4, pp. 289-294.

Wassermann, S., Feder, D., Abdel-Maksoud, M., 2016a, "Estimation of ship roll damping – A comparison of the decay and the harmonic excited roll motion technique for a post panamax containership", Ocean Engineering, 120, pp. 371-382.

Wassermann, S. Krambs, G., Abdel-Maksoud, M., 2016b, "Estimation of force coefficients for normal forces on bilge keels and skin friction roll damping of ships by CFD simulations", Proceedings of the 15th International Ship Stability Workshop, Sweden.

Watanabe, Y, 1930, "On the Design of Anti-rolling Tanks", Journal of Zosen Kiokai, the Society of Naval Architects of Japan, Vol. 46, pp. 125-153 (in Japanese).

Watanabe, Y, 1943, "On the Design of frahm type Anti rolling Tank", Bulletin of Zosen Kiokai, the Society of Naval Architects of Japan, Vol.258, pp. 251-255(in Japanese).

Appendix A. SIMPLIFIED IKEDA'S METHOD FACTORS

Table 1 Factors Q1 and Q2

Factor Q1					
	1	**2**	**3**	**4**	**5**
1	0.00000	0.00000	0.00000	0.00000	0.00000
2	0.00000	-0.002222	0.040871	-0.286866	0.599424
3	0.00000	0.010185	-0.161176	0.904989	-1.641389
4	0.00000	-0.015422	0.220371	-1.084987	1.834167
5	-0.0628667	0.4989259	0.52735	-10.7918672	16.616327
6	0.1140667	-0.8108963	-2.2186833	25.1269741	-37.7729778
7	-0.0589333	0.2639704	3.1949667	-21.8126569	31.41135
8	0.0107667	0.0018704	-1.2494083	6.9427931	-10.2018992
9	0.00000	0.192207	-2.787462	12.507855	-14.764856
10	0.00000	-0.350563	5.222348	-23.974852	29.007851
11	0.00000	0.237096	-3.535062	16.368376	-20.539908
12	0.00000	-0.067119	0.966362	-4.407535	5.894703
13	0.00000	17.945	-166.294	489.799	-493.142
14	0.00000	-25.507	236.275	-698.683	701.494
15	0.00000	9.077	-84.332	249.983	-250.787
16	0.00000	-16.872	156.399	-460.689	463.848
17	0.00000	24.015	-222.507	658.027	-660.665
18	0.00000	-8.56	79.549	-235.827	236.579
Factor Q2					
	0.00000	-1.402	7.189	-10.993	9.45

Table 2 Factor Q3

Factor Q3				
	1	**2**	**3**	**4**
1	-7686.0287	30131.5678	-49048.9664	42480.7709
2	61639.9103	-241201.0598	392579.5937	-340629.4699
3	-130677.4903	507996.2604	-826728.7127	722677.104
4	-110034.6584	446051.22	-724186.4643	599411.9264
5	709672.0656	-2803850.2395	4553780.5017	-3888378.9905
6	-822735.9289	3238899.7308	-5256636.5472	4500543.147
7	299122.8727	-1175773.1606	1907356.1357	-1634256.8172
Factor Q3				
	5	**6**	**7**	
1	-20665.147	5355.2035	-577.8827	
2	166348.6917	-43358.7938	4714.7918	
3	-358360.7392	95501.4948	-10682.8619	
4	-264294.7189	58039.7328	-4774.6414	
5	1839829.259	-457313.6939	46600.823	
6	-2143487.3508	538548.1194	-55751.1528	
7	780020.9393	-196679.7143	20467.0904	

Table 3 Factors Q4 and Q5

Factor Q4				
	1	**2**	**3**	**4**
1	-0.3767	3.39	-10.356	11.588
2	-17.109	41.495	-33.234	8.8007
3	36.566	-89.203	71.8	-18.108
4	0	-0.0727	0.7	-1.2818
Factor Q5				
Index	**1**	**2**	**3**	**4**
Q5	-1.05584	12.688	-63.70534	172.84571
Index	**5**	**6**	**7**	**8**
Q5	-274.05701	257.68705	-141.40915	44.13177
Index	**9**	**10**	**11**	**12**
Q5	-7.1654	-0.0495	0.4518	-0.61655

Table 4 Factor Q6

Factor Q6					
	1	**2**	**3**	**4**	**5**
1	-79.414	215.695	-215.883	93.894	-14.848
2	0.9717	-1.55	0.723	0.04567	0.9408
3	0	-219.2	443.7	-283.3	59.6

Table 5 Factor Q7

Factor Q7			
	1	**2**	**3**
1	0	-0.3651	0.3907
2	0	-2.21	2.632
3	0.00255	0.122	0.4794
4	-0.8913	-0.0733	0
5	5.2857	-0.01185	0.00189
6	0.00125	-0.0425	-1.86
7	-0.0657	0.0586	1.6164